Natural Radiocarbon in the Atlantic Ocean[1]

WALLACE S. BROECKER, ROBERT GERARD, MAURICE EWING, AND BRUCE C. HEEZEN

Lamont Geological Observatory
Columbia University
Palisades, New York

Abstract. By the use of suitable chemical and radiometric techniques the natural radiocarbon concentration in the dissolved bicarbonate of 135 samples representing the major water masses of the Atlantic Ocean has been determined with a precision ranging from 0.5 to 1.3 per cent. Whereas the results from a given water mass exhibit a standard deviation only slightly exceeding that predicted from the experimental error alone, measurable differences exist between the major water masses, the total range in C^{14}/C^{12} ratio being about 10 per cent. Corrections for the bomb-produced C^{14} effect and the industrial CO_2 effect have been applied where necessary.

The surface water C^{14}/C^{12} ratios show a progressive increase from south to north, ranging from 120 per mil lower than the preindustrial atmospheric value in the Antarctic to 50 per mil lower in the North Atlantic. Deep water masses originating in the high latitudes of the southern hemisphere have consistently lower C^{14}/C^{12} ratios than those originating in the high latitudes of the northern hemisphere. A layer of water of high C^{14}/C^{12} ratio found at depths between 1200 and 2400 meters in the western North Atlantic may well represent a wedge of young water penetrating the older North Atlantic deep water. Bottom water in the eastern basin of the North Atlantic has a 20 per mil lower C^{14}/C^{12} ratio than the corresponding water in the western basin.

According to a steady-state circulation model, most of the water below 600 meters in the North Atlantic remains at depth for an average of 650 years. Corresponding residence times for water masses of Antarctic origin are less than 350 years.

A circulation model explaining the prominent features of the C^{14} distributions in the atmosphere-ocean system is based on a south to north transport of water along the surface of the Atlantic Ocean, with a return flow at depth. The Atlantic and Pacific communicate through the Antarctic. On the basis of this model, despite the lower ΔC^{14} values, the mean residence times of water in the deep reservoirs of the Pacific may not exceed those for the deep Atlantic by more than 30 per cent.

Although results of C^{14} analyses on tree rings suggest that the oceans are reasonably close to steady state, the possibility of nonsteady-state circulation must be considered. It is shown that the present C^{14} distribution in the oceans could be achieved through the storage of C^{14} in the atmosphere and surface oceans during a relatively short period of greatly restricted bottom water formation. If nonequilibrium effects are important the residence times computed from the steady-state model could be considerably in error.

Introduction. The absolute rate of overturn of waters in the deep ocean is of considerable interest not only to the oceanographer but also to those engaged in other branches of earth science. For example, because of the large heat capacity of the deep sea, its rate of interaction with the surface ocean and atmosphere is of major interest to the meteorologist and the climatologist. The biologist interested in the cycle of nutrients in the ocean also needs esti-

mates of residence times in the deep sea. More recently those concerned with the problem of radioactivity produced by bombs and reactors have looked to the oceans as a diluent for these products. Again, mixing rates are of prime importance.

Although considerable progress has been made in understanding the patterns and rates of mixing in the oceans by traditional studies of density distribution, the problem is an exceedingly complex one, requiring as many independent approaches as possible. One such approach, the study of the distribution of C^{14} in the oceans,

was first applied in 1950 by Ewing and Kulp. The original C^{14} measurements reported by *Kulp, Tryon, Eckelmann, and Snell* [1952] were later found to be somewhat in error owing to contamination in the ascarite absorbent used in shipboard processing and to the inherent problems of the black carbon assay system. These results, however, showed that the residence time for deep waters in the Atlantic Ocean was less than 2000 years. In 1955 the present study was initiated at Lamont. A new water processing system and the more precise gas counting assay technique [*Broecker, Tucek, and Olson*, 1959] were used. Preliminary results of this investigation have been given by *Broecker* [1957] and *Broecker, Ewing, Gerard, Heezen, and Kulp* [1958]. Other laboratories are also currently carrying out similar studies. Results of these investigations have been published by *Rafter* [1955], *Rafter and Fergusson* [1958], *Brodie and Burling* [1958], *Garner* [1958], *Rubin and Alexander* [1958], *Fonselius and Ostlund* [1959], and *Suess, Rakestraw, and Oeschger* [1959]. The work reported here was carried out as a joint project between the geophysics and geochemistry groups at Lamont, the former being responsible for the design of the water sampler and the collection and shipboard chemical processing of the water samples and the latter for the design of the shipboard processing system and the laboratory analysis of samples.

The object of the present research was to determine the geographic and depth variation in the Atlantic Ocean of the ratio of C^{14} (a radioactive isotope of 5570 years half-life), to C^{13} (the most abundant stable isotope of carbon). If it is assumed that factors other than the radioactive decay producing these variations could be recognized and accounted for, then the residual differences should be related to mixing rates.

Experimental techniques. The procedures for sampling sea water for C^{14} have been designed to collect large-volume samples from accurately known depths in the ocean, to extract the inorganic carbon in the form of CO_2, and to return that portion, free from contamination, to the laboratory for C^{14}/C^{13} measurements.

The total concentration of inorganic CO_2 in all forms in ocean water is about 0.025 grams of carbon per liter [*Sverdrup, Johnson, and Fleming*, 1942]. The volume of the Lamont counters

for measuring C^{14} content is 5 liters. Five grams of carbon in form of CO_2 gas is required to produce 2 atmospheres of pressure in the counters. On the basis of this requirement, a minimum of 200 liters of sea water is needed for each sample. During the period 1955–1959 400-liter samples were collected to allow for variations in the efficiency of the recovery system. Currently, a 220 liter sampler is sufficient because of improvements in recovery techniques.

Both types of sampler were designed to be lowered into the ocean by a winch using $\frac{1}{2}$-inch wire rope to which the sampler is securely attached. The lowering is accomplished with a 1500-pound piston-coring device fixed to the wire rope below the water sampler as a weight. The earlier 400-liter sampler consisted of a rigid steel barrel with two round, 10-inch-diameter ports at the top fitted with hinged doors which opened and closed in unison. As the sampler was lowered through the water a hood-like baffle directed the flow of water into one of the open ports while a partition inside the sampler further directed the flow to the bottom of the barrel, from whence the water moved up and out of the other open port. Dye experiments have shown that, with this method of flushing, less than 0.1 per cent of an original water volume remains in the sampler after it is lowered 100 meters. The same principle is used in the present sampler (Fig. 1) but it has only one door which when open divides the single port in two and when closed seals the port with an O-ring seal.

When the sampler is lowered to the desired depth, a 'messenger' in the form of a 5-pound weight is dropped down the wire from the surface. The messenger strikes a release on the sampler which closes the doors. In order to interpret the results with respect to water masses in the ocean, precise knowledge of depth of sampling is necessary. To afford additional control to that provided by length and angle of wire and by sounding, protected and unprotected reversing thermometers are used inside the barrel. When the door closes, the thermometers reverse, thereby indicating the depth and temperature of the sample. A small Bourdon-tube recorder is also used to indicate the depth of closing of the sampler door.

When the sampler is brought up to the sur-
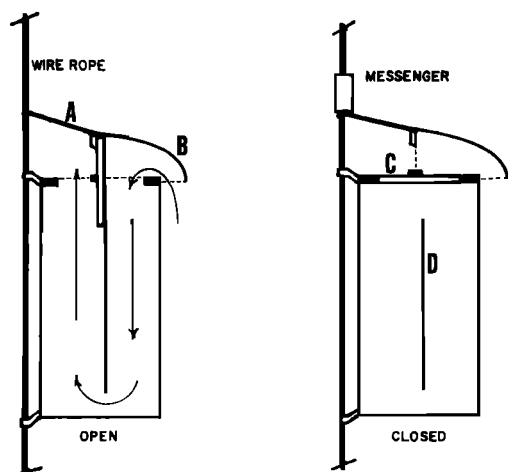
LARGE-VOLUME WATER SAMPLER

Fig. 1. Idealized diagram of 220-liter water sampler presently in use. The drawing on the left shows the open position. Arm A is the trigger arm which releases the closing mechanism. Hood B directs the flow of water into the barrel while lowering. The drawing on the right shows the sampler in closed position. Round plastic door C has an "O" ring seal and closes when messenger strikes trigger arm A. Partition D channels water to bottom of sampler to aid circulation while lowering.

face, samples are taken for determination of salinity and dissolved oxygen. A submersible pump is then placed in the bottom of the barrel and the water is pumped through a hose to a plastic deck tank where processing for removal of CO_2 is carried out.

The water in the processing tank is acidified with H_2SO_4 and bubbled in a closed system with CO_2-free air or tank N_2. In the present system, greater CO_2 recovery is achieved by using a pump to circulate the water within the tank and to spray it into the gas phase. The CO_2 released to the gas phase is absorbed in $5N$ KOH held in two 1-liter bubblers operated in series. Recovery of 70 per cent of the CO_2 from a 220-liter sample now takes about 3 hours. The recovery is monitored by means of a titration technique. The KOH is returned to the laboratory, where it is acidified again and the CO_2 is released. The CO_2 is purified by absorption and desorption from CaO contained in quartz tubes and is then assayed for radioactivity in a 5-liter proportional counter. The precision of the C^{14} assay

ranges from 0.5 to 1.0 per cent, except in some of the early measurements in which the errors ranged up to 1.5 per cent. The ratio of stable C^{13} to C^{12} in the purified CO_2 gas is determined with a precision of 0.1 per cent using a model 201 Consolidated Electrodynamics double-collecting mass spectrometer. The details of this procedure have been published separately [*Broecker, Tucek, and Olson,* 1959].

The results (Table 1) are ultimately expressed as per mil differences from a standard; the exact expression is

$$\delta C^{14} = \frac{A_{sample}{}^* - 0.950 A_{standard}{}^\circ}{0.950 A_{standard}{}^\circ} \times 1000$$

where $A_{sample}{}^*$ is the net C^{14} activity of the sample corrected for radioactive decay between the time of collection (or formation, in the case of tree ring samples) and measurement and $A_{standard}{}^\circ$ is the net C^{14} activity of the National Bureau of Standards oxalic acid standard corrected for radioactive decay between January 1, 1958, and the time of measurement. The factor 0.950 is a defined constant introduced to place the zero on the δC^{14} scale close to the value of 19th century wood samples. In order to eliminate differences introduced by fractionation, the results are normalized to a common C^{13}/C^{12} ratio. The normalization equation is

$$\Delta C^{14} = \delta C^{14}$$
$$- 2 \, \delta C^{13}(1 + (\delta C^{14}/1000)) - 50.0$$

where δC^{14} is defined as above and

$$\delta C^{13} = \frac{R_{sample} - R_{belemnite\ standard}}{R_{belemnite\ standard}} \times 1000$$

where R stands for C^{13}/C^{12} ratio. The constant factor (-50.0) is introduced in order to place the zero on the scale at a convenient point (the C^{14}/C^{12} ratio corrected in age to pre-1900 wood samples).

The normalization of the results to a common δC^{13} value is of considerable convenience. Not only does it remove differences introduced by fractionation during chemical processing but it also allows results from various materials (i.e., atmospheric CO_2, ocean $HCO_3{}^-$, and organic materials) to be directly compared as if they had formed within a system free of isotope

fractionation effects. (See *Broecker and Olson* [1959] for a more complete discussion of the derivation of the above scale and of its use.)

The δC^{13} results show a considerable scatter around the rather uniform value of about -2 per mil found for ocean water by several other workers. Much of this scatter is the result of poor gas dispersion with consequent lowering of the efficiency of CO_2 recovery in some of the KOH bubblers used in shipboard processing. As shown by *Craig* [1953], during uptake by basic solutions the lighter isotopes are more efficiently captured by the solution. Of the samples reported in this paper those showing poor chemical yield are the ones for which large negative δC^{13} values were observed. In general a rather consistent relationship between δC^{13} and yield is apparent. For 30 of the 135 analyses reported, no δC^{13} values are available. In these cases values have been estimated from yield data and from δC^{13} results on other samples from the same cruise. The errors on the ΔC^{14} values computed have been increased in order to cover the uncertainty in these estimates. Since the C^{14} fractionation will always be twice the C^{13} fractionation, no significant error is introduced in cases where mass-spectrometer measurements are available.

Results. Since 1955, radiocarbon measurements have been made on over 130 sea water samples collected by Lamont workers aboard the research vessel *Vema* in the North and South Atlantic oceans. The results of these measurements are given in Table 1.

On the basis of the findings of numerous oceanographic surveys over the past 35 years, beginning with the *Meteor* expedition, the Atlantic has become the best known of the world's oceans. The broad features of the distribution of water masses and the general circulation of the North and South Atlantic have been summarized by *Sverdrup, Johnson, and Fleming* [1942] and *Sverdrup* [1954]. These features, based on the observed distribution of conservative properties, allow the vertical and areal extent of the different water masses, their surface sources, and some of their mixing characteristics to be defined.

The major water masses described in these studies of the Atlantic may be listed as follows:

North Atlantic Central Water (NACW). This water mass lies beneath the surface mixed layer in the central North Atlantic between the depths of 100 and 700 meters. Characterized by relatively high temperature and salinity, it lies within the great gyre of surface circulation bounded on the west by the Gulf Stream, on the north by the North Atlantic Current, on the east by the Canary Current, and on the south by the North Equatorial Current. The boundaries of this mass lie between temperatures of 8°C and 19°C and salinities of 35.1 per mil to 36.7 per mil. Unlike the deeper masses, rather steep temperature and salinity gradients exist between the top and bottom of the mass, suggesting an origin through the mixing of a warm and a cold water mass of different salinity. Whether this mixing occurs at the source or at depth is not known; the resultant gradient could be explained equally well by either process.

South Atlantic Central Water (SACW). This water mass is the southern-hemisphere counterpart of the NACW, although somewhat shallower in vertical extent, lying between 100 and 600 meters. The water has a vertical decrease in temperature ranging from 6° to 18°C and in salinity from 34.5 to 36.0 per mil. This water outcrops at the surface in a zone known as the Subtropical Convergence, extending along latitude 40°S, and can be traced at depth throughout the South Atlantic to the equator.

Antarctic Intermediate Water (AAIW). Water of this description is thought to form along a conspicuous circumpolar belt (in the southern ocean) known as the Antarctic Convergence. In the South Atlantic this convergence lies along latitude 50°S. Here water of $\sim 3°C$ temperature and salinity of ~ 34 per mil sinks and moves northward at depths centered at 700 to 800 meters. This water can easily be identified as to origin, having a lower salinity than surrounding waters. As it moves northward it mixes with waters above and below, gradually attaining higher temperature and salinity. Traces of AAIW can be observed in the western North Atlantic as far north as 30°N.

Antarctic Bottom Water (AABW). Water formed in the Weddell Sea area of the Antarctic has the highest density of all ocean water. This water can be traced in the western basin of the Atlantic beginning at a temperature of about 0°C and a salinity of 36.65 per mil in the

TABLE 1. Sample Locations and Radiocarbon Results

Date Collected	Latitude	Longitude	Sample Depth, meters	Bottom Depth, meters	Temp, °C	Salinity, ‰	Water Type†	δC^{14}, ‰	δC^{13},‡ ‰	ΔC^{14},‡ ‰	Index No.
I. Surface Water, 0–50 meters											
A. North Atlantic											
10/30/55	38°22′N	71°32′W	0	2910	17.9		Gulf Stream	−9 ± 7	+1.8	−62 ± 7	1
7/19/55	37°58′N	50°53′W	0	5423	24.9	36.35	North Atlantic Current	+12 ± 8	(−2.0)	(−34 ± 10)	2
11/ 1/55	36°06′N	66°06′W	0	5158	23.1		Sargasso Sea	−5 ± 6	−1.1	−52 ± 7	3
11/ 3/55	34°06′N	65°06′W	0	5069	24.8		Sargasso Sea	+4 ± 6	(+5.0)	(−56 ± 8)	4
11/13/57	34°05′N	65°00′W	0	4726	22.2		Sargasso Sea	−1 ± 5	+1.5	−54 ± 5	5
6/ 2/56	33°50′N	66°18′W	0	5114	21.7		Sargasso Sea	−5 ± 5	+2.2	−59 ± 5	6
6/ 7/56	33°00′N	49°48′W	0	4667	22.3		Sargasso Sea	−6 ± 6	+0.7	−58 ± 6	7
6/ 5/56	32°38′N	57°55′W	0	5218	22.7		Sargasso Sea	+9 ± 6	+1.4	−44 ± 6	8
6/12/56	31°45′N	34°38′W	0	3878	21.9		Sargasso Sea	−13 ± 7	(+1.0)	(−65 ± 10)	9
11/16/57	29°57′N	61°41′W	0	2748	23.3		Sargasso Sea	+26 ± 5	(+5.0)	(−34 ± 8)	10
11/17/57	29°13′N	60°30′W	46	5836	24.2	36.56	Sargasso Sea	+13 ± 6	−1.8	−33 ± 6	11
11/ 5/55	27°05′N	73°32′W	0	4717	25.1		Sargasso Sea	+5 ± 6	+4.9	−55 ± 6	12
6/24/57	25°42′N	79°23′W	0	…	…		Antilles Current	−2 ± 7	+2.3	−44 ± 7	13
11/ 8/55	25°25′N	75°13′W	0	4561	26.1		Florida Current	+6 ± 5	+0.8	−45 ± 5	14
11/12/55	20°32′N	68°30′W	0	5091	27.8		Antilles Current	+10 ± 10	+2.0	−44 ± 10	15
11/10/55	19°58′N	70°53′W	0	1801	28.2		Antilles Current	+14 ± 7	+7.5	−51 ± 7	16
11/14/55	19°07′N	67°07′W	0	4973	27.8		Antilles Current	+8 ± 5	+2.1	−46 ± 5	17
11/26/57	15°03′N	39°48′W	0	5222	26.7		North Equatorial Current	+1 ± 8	−1.0	−47 ± 8	18
B. Caribbean											
12/20/55	19°04′N	80°48′W	0	1324	27.3		West Caribbean	−1 ± 7	(+3.0)	(−57 ± 9)	19
12/10/55	16°17′N	79°14′W	0	798	27.6		West Caribbean	−11 ± 10	+7.2	−76 ± 10	20
12/16/55	17°39′N	79°04′W	0		…		West Caribbean	−5 ± 7	−1.1	−53 ± 7	21
12/ 8/55	12°27′N	77°25′W	0	3918	27.8		East Caribbean	+9 ± 6	+2.3	−46 ± 6	22
11/25/55	17°05′N	71°36′W	0	2075	27.8		East Caribbean	+9 ± 7	+5.5	−52 ± 7	23
11/19/55	16°43′N	70°38′W	0	4101	27.8		East Caribbean	+4 ± 7	+4.6	−55 ± 7	24
11/17/55	17°11′N	68°55′W	0	5567	27.4		East Caribbean	−1 ± 6	+5.1	−61 ± 6	25
11/22/55	17°47′N	68°22′W	0	2536	27.8		East Caribbean	+11 ± 7	+5.9	−51 ± 7	26
C. Mediterranean											
8/16/56	34°04′N	26°21′E	0	3181	26.0		E. Mediterranean	−4 ± 7	+4.2	−63 ± 7	27
7/24/56	38°06′N	22°54′E	0	795	25.2		Gulf of Corinth	−53 ± 7	−2.3	−99 ± 7	28

TABLE 1. Continued

Date Collected	Latitude	Longitude	Sample Depth, meters	Bottom Depth, meters	Temp,* °C	Salinity,* ‰	Water Type†	δC^{14}, ‰	δC^{13},‡ ‰	ΔC^{14},‡ ‰	Index No.
D. South Atlantic											
12/ 5/57	00°51'N	32°52'W	49	3303	26.9	36.08	South Equatorial Current	−28 ± 6	−1.1	−76 ± 6	29
2/15/56	03°06'S	32°26'W	0	4228	27.6		South Equatorial Current	−2 ± 6	+1.4	−55 ± 6	30
2/17/56	03°34'S	31°22'W	0	4411	26.9		South Equatorial Current	−13 ± 7	(+1.0)	(−61 ± 10)	31
1/ 9/57	04°29'S	34°54'W	0	3371	27.1		South Equatorial Current	−24 ± 5	−0.4	−73 ± 5	32
5/20/57	05°41'S	10°39'E	0	2087	27.5		North Benguela Current	−24 ± 7	−3.3	−68 ± 7	33
12/16/57	09°38'S	34°05'W	0	4707	27.2		Brazil Current	−8 ± 7	(−1.0)	(−56 ± 9)	34
1/19/57	10°59'S	32°28'W	0	4978	27.2		Brazil Current	−11 ± 7	−4.2	−52 ± 7	35
12/26/57	23°12'S	37°38'W	0	3824	26.4		Brazil Current	+7 ± 7	−2.1	−39 ± 7	36
5/12/57	14°30'S	07°34'E	0	3985	24.4		Central South Atlantic	−10 ± 15	(−1.0)	(−58 ± 15)	37
5/ 5/57	22°34'S	14°12'E	73	Plankton sample			Central South Atlantic	−64 ± 15	−16.0	−84 ± 15	38
5/ 3/57	25°31'S	12°26'E	0	3030	17.9		Central South Atlantic	−13 ± 5	−1.3	−60 ± 5	39
4/29/57	32°13'S	16°20'E	0	455	19.3		Central South Atlantic	−2 ± 7	−0.9	−51 ± 7	40
4/ 6/58	34°06'S	18°06'E	0	188	20.0		Central South Atlantic	−8 ± 6	−1.2	−56 ± 6	41
4/19/57	34°46'S	06°29'E	0	5308	17.0		West Benguela	−2 ± 7	−5.1	−42 ± 7	42
4/ 6/57	39°03'S	41°48'W	0	5112	17.8		West Wind Drift	−2 ± 5	+1.0	−54 ± 5	43
4/12/57	40°54'S	20°29'W	0	3351	12.3		West Wind Drift	−21 ± 7	−6.6	−58 ± 7	44
4/15/57	41°15'S	06°10'W	0	4085	12.3		West Wind Drift	−14 ± 7	−2.2	−59 ± 7	45
4/ 2/57	40°43'S	56°32'W	0	1022	11.1		Falkland Current	−27 ± 5	+0.6	−79 ± 5	46
4/ 3/57	41°05'S	51°09'W	0	5506	16.6		Falkland Current	−27 ± 7	−1.6	−74 ± 7	47
3/20/57	45°24'S	59°13'W	0	1726	9.0		Falkland Current	−27 ± 6	+0.3	−78 ± 6	48
E. Antarctic											
3/24/58	51°27'S	02°38'E	0	3329	3.5		Antarctic Convergence	−28 ± 6	+5.6	−88 ± 6	49

TABLE 1. Continued

Date Collected	Latitude	Longitude	Sample Depth, meters	Bottom Depth, meters	Temp.,* °C	Salinity,* ‰	Water Type†	δC^{14}, ‰	δC^{13},‡ ‰	ΔC^{14},‡ ‰	Index No.
2/24/58	55°27'S	57°10'W	0	1750	3.0		Drake Passage	−69 ± 7	−4.2	−111 ± 7	50
3/19/58	57°07'S	07°15'W	0	3444	1.0		Antarctic Surface Water	−79 ± 5	−4.9	−120 ± 5	51

II. *Subsurface Water, below 50 m*
A. *200–400 meters*

Date Collected	Latitude	Longitude	Sample Depth, meters	Bottom Depth, meters	Temp.,* °C	Salinity,* ‰	Water Type†	δC^{14}, ‰	δC^{13},‡ ‰	ΔC^{14},‡ ‰	Index No.
4/16/56	25°01'N	59°12'W	256	6081	(18)	(36.6)	NACW	−11 ± 7	+3.1	−67 ± 7	52
10/12/56	23°22'N	27°14'W	329	5499	(16)	36.08	NACW	−15 ± 5	+4.2	−74 ± 5	53
4/11/56	15°49'N	47°12'W	229	3757	(16)	(36.2)	NACW	−29 ± 6	−2.6	−73 ± 6	54
4/7/56	08°15'N	37°54'W	274	3520	(9)	(34.9)	Transition NACW–SACW	−49 ± 9	−2.9	−93 ± 9	55
12/3/57	07°22'N	29°59'W	240	4894	(9)	35.10	Transition NACW–SACW	−41 ± 6	−0.9	−89 ± 6	56
6/9/57	00°19'S	24°29'W	201	2988	13.5	(35.2)	SACW	−18 ± 7	−2.4	−63 ± 7	57
2/16/56	03°17'S	32°14'W	274	4433	(10)	34.91	SACW	−35 ± 7	−0.4	−84 ± 7	58
5/19/57	06°25'S	11°26'W	366	439	10.1	(35.0)	Lower SACW	−38 ± 7	−2.5	−83 ± 7	59
12/21/57	14°02'S	37°32'W	295	3804	16.35	35.71	SACW	−8 ± 5	−1.9	−55 ± 5	60
12/21/57	14°10'S	37°33'W	300	3749	(15)	35.37	SACW	−4 ± 6	+1.6	−57 ± 6	61
5/9/57	21°14'S	03°22'E	Surface to 274	5134	(11)	(34.9)	SACW	−13 ± 7	−1.5	−60 ± 7	62
5/2/57	28°26'S	08°39'E	201	5066	(14)	(35.3)	SACW	−4 ± 7	−2.5	−49 ± 7	63

B. *500–1200 meters*

Date Collected	Latitude	Longitude	Sample Depth, meters	Bottom Depth, meters	Temp.,* °C	Salinity,* ‰	Water Type†	δC^{14}, ‰	δC^{13},‡ ‰	ΔC^{14},‡ ‰	Index No.
7/19/55	38°00'N	51°37'W	732	5405	(12)	35.95	Lower NACW	+7 ± 13	(−2.0)	(−39 ± 13)	64
10/11/56	24°23'N	24°03'W	1097	5104	(7)	35.18	N. Atlantic Undefined	−41 ± 10	+8.5	−107 ± 10	65
6/17/55	23°28'N	65°56'W	896		(8)	35.12	N. Atlantic Undefined	−50 ± 13	(−2.0)	(−96 ± 13)	66
4/14/56	22°22'N	54°19'W	823	5654	(8)	(35.0)	N. Atlantic Undefined	−49 ± 6	(−2.0)	(−95 ± 8)	67
11/22/57	20°44'N	49°24'W	950	4354	6.0	34.97	N. Atlantic Undefined	−57 ± 6	−14.8	−79 ± 6	68
12/25/55	19°09'N	76°59'W	1097	3749	(5)	34.84	N. Atlantic Undefined	−43 ± 7	−1.3	−91 ± 7	69
4/11/56	15°49'N	47°12'W	823	3757	(6)	(34.7)	N. Atlantic Undefined	−50 ± 6	0.0	−100 ± 6	70
11/26/57	15°29'N	40°30'W	823	4330	6.1	34.85	N. Atlantic Undefined	−73 ± 6	−7.1	−110 ± 6	71

TABLE 1. Continued

Date Collected	Latitude	Longitude	Sample Depth, meters	Bottom Depth, meters	Temp.,* °C	Salinity,* ‰	Water Type†	δC14, ‰	δC13,† ‰	ΔC14,† ‰	Index No.
4/ 7/56	08°14'N	37°48'W	823	3598	(5)	(34.7)	N. Atlantic Undefined	−60 ± 5	−0.1	−110 ± 5	72
12/ 5/57	00°51'N	32°52'W	799	3314	(4.3)	34.60	AAIW	−63 ± 6	−1.3	−111 ± 6	73
2/16/56	03°22'S	31°50'W	732	4301	(4.4)	34.46	AAIW	−76 ± 6	−0.2	−125 ± 6	74
5/26/57	04°47'S	02°40'E	732	5238	(5)	(34.5)	AAIW	−64 ± 7	−12.7	−90 ± 7	75
12/16/57	10°04'S	33°52'W	914	4625	(4.0)	34.65	AAIW	−86 ± 6	−0.7	−134 ± 6	76
5/ 9/57	21°09'S	03°20'E	550	5084	5.96	(34.5)	Upper AAIW	−67 ± 7	−2.1	−113 ± 9	77
5/ 2/57	28°25'S	08°36'E	1189	5060	3.5	(34.5)	Lower AAIW	−92 ± 7	−2.4	−137 ± 7	78
C. 1200–2500 meters											
10/31/57	39°16'N	70°46'W	2323	2642	3.2	34.88	Upper NADW	−22 ± 5	−2.2	−68 ± 5	80
7/19/55	37°58'N	50°53'W	1944	5423	3.69	34.88	Upper NADW	−19 ± 7	(−2.0)	(−65 ± 13)	81
11/17/57	29°13'N	60°31'W	1423	5843	4.75	35.25	Upper NADW	−32 ± 10	(−3.0)	(−76 ± 10)	82
6/15/55	25°07'N	69°57'W	1829	5504	(3.8)	34.94	Upper NADW	−20 ± 13	−1.7	−67 ± 13	83
11/ 4/57	20°31'N	73°22'W	1230	3260	(4)	(35.0)	Upper NADW	−5 ± 6	−2.7	−49 ± 6	84
7/ 4/57	11°12'N	59°19'W	2305	4113	(3)	(35.0)	Upper NADW	−61 ± 7	−13.0	−88 ± 7	87
7/ 4/57	11°12'N	57°16'W	1765	4114	(4)	(35.0)	Upper NADW	−43 ± 6	−5.6	−83 ± 6	88
7/ 3/57	10°49'N	55°41'W	1262	4396	(5)	(34.9)	Upper NADW	−62 ± 6	−15.9	−83 ± 6	89
10/10/56	25°13'N	21°23'W	1463	4548	(5)	35.07	Upper NADW	−56 ± 5	−0.7	−104 ± 5	90
9/10/56	25°13'N	21°23'W	1829	4656	(4.5)	35.08	Upper NADW	−60 ± 6	+0.3	−111 ± 6	91
4/ 7/56	08°15'N	37°53'W	1463	3598	(4)	(35.0)	Upper NADW	−53 ± 7	+2.5	−108 ± 7	92
5/27/57	04°23'S	00°05'W	1829	4799	3.8	(34.96)	Upper NADW	−47 ± 6	−0.8	−96 ± 6	93
12/16/57	10°06'S	34°54'W	1829	4625	3.83	34.96	Upper NADW	−54 ± 8	−0.9	−102 ± 8	94
12/17/57	12°37'S	35°00'W	1829	4378	(3.7)	34.96	Upper NADW	−55 ± 9	−6.6	−92 ± 9	95
12/22/57	15°17'S	36°00'W	1900	4369	3.6	34.94	Upper NADW	−61 ± 7	+0.4	−112 ± 7	96
5/ 8/57	22°40'S	03°16'E	1646	5046	(3.2)	(34.8)	Antarctic and NADW	−80 ± 10	−3.3	−124 ± 10	97
4/ 2/57	35°20'S	10°42'E	2195	5008	(2.8)	(34.8)	Antarctic and NADW	−71 ± 10	+0.7	−122 ± 10	98
4/ 7/57	38°58'S	40°06'W	1829	5103	2.98	(34.7)	Antarctic and NADW	−100 ± 5	−4.3	−143 ± 5	99
D. 2500–4000 meters											
7/27/55	34°55'N	57°11'W	3488	3671	2.70	34.91	NADW	−43 ± 10	(−2.0)	(−89 ± 10)	100
4/18/56	28°41'N	60°19'W	2560	5528	(3.3)	(34.95)	NADW	−62 ± 6	+0.9	−114 ± 6	101
9/ 9/56	26°10'N	18°06'W	3503	3548	(2.6)	34.91	NADW	−62 ± 8	+0.6	−113 ± 8	102
4/16/56	25°01'N	59°11'W	2560	6081	(3.3)	(34.95)	NADW	−56 ± 7	+0.9	−108 ± 7	103
6/22/55	24°26'N	70°23'W	2787	5534	(3.0)	(34.95)	NADW	−50 ± 7	(−2.0)	(−96 ± 9)	104

TABLE 1. Continued

Date Collected	Latitude	Longitude	Sample Depth, meters	Bottom Depth, meters	Temp,* °C	Salinity,* ‰	Water Type†	δC¹⁴, ‰	δC¹³,‡ ‰	ΔC¹⁴,‡ ‰	Index No.
11/21/57	22°03′N	51°27′W	2700	5050	2.98	34.96	NADW	−53 ± 6	−5.3	−93 ± 6	105
11/22/57	20°43′N	49°26′W	2926	4058	2.92	34.96	NADW	−62 ± 6	−1.3	−110 ± 6	106
11/25/57	16°44′N	42°38′W	3840	4502	2.46	34.92	NADW	−69 ± 7	−3.9	−112 ± 7	107
12/31/56	15°52′N	38°03′W	3840	5300	(2.5)	34.95	NADW	−53 ± 5	−9.6	−85 ± 5	108
4/11/56	15°49′N	47°12′W	2560	3757	(3.0)	(34.95)	NADW	−74 ± 7	+3.1	−130 ± 7	109
2/18/55	03°48′S	30°53′W	2560	4426	(2.9)	(34.95)	NADW	−49 ± 6	−1.0	−97 ± 6	110
5/27/57	04°23′S	00°15′W	2743	4779	2.8	(34.89)	NADW	−62 ± 7	−1.3	−110 ± 7	111
1/22/57	17°03′S	28°13′W	2807	5141	(2.75)	34.93	NADW	−71 ± 6	−8.3	−106 ± 6	112
5/ 8/57	22°56′S	04°52′E	2560	2824	(2.75)	(34.88)	NADW	−63 ± 7	−3.8	−106 ± 7	113
1/18/58	38°25′S	53°11′W	2770	2908	2 75	34.89	NADW	−57 ± 6	−2.3	−103 ± 6	114
E, >4000 meters											
7/16/55	39°27′N	56°57′W	4345	5260	2.32	34.80	NADW (W. Basin)	−43 ± 7	(−2.0)	(−89 ± 9)	115
7/18/55	39°03′N	53°29′W	5281	5317	2.26	(34.9)	NADW (W. Basin)	−58 ± 7	(−2.0)	(−104 ± 9)	116
7/19/55	38°00′N	51°37′W	5369	5405	2.31	34.80	NADW (W. Basin)	−40 ± 13	(−2.0)	(−86 ± 13)	117
7/23/55	37°23′N	53°22′W	5368	5404	2.25	34.80	NADW (W. Basin)	−73 ± 13	(−2.0)	(−119 ± 13)	118
7/26/55	35°28′N	55°48′W	5416	5452	2.60	34.80	NADW (W. Basin)	−53 ± 7	(−2.0)	(−99 ± 9)	119
7/22/55	35°43′N	53°15′W	5454	5490	2.25	34.80	NADW (W. Basin)	−58 ± 5	(−2.0)	(−104 ± 9)	120
7/21/55	34°46′N	52°46′W	5481	5517	(2.2)	34.81	NADW-(AABW)	−76 ± 13	(−2.0)	(−122 ± 13)	121
6/27/55	31°47′N	71°13′W	5360	5405	2.16	34.80	NADW-(AABW)	−60 ± 13	(−2.0)	(−106 ± 13)	122
6/29/55	31°21′N	66°39′W	4893	4938	2.22	34.86	NADW-(AABW)	−56 ± 7	(−2.0)	(−102 ± 9)	123
6/27/55	31°17′N	71°13′W	5367	5412	2.19	35.17	NADW-(AABW)	−52 ± 9	(−2.0)	(−98 ± 10)	124
6/26/55	29°14′N	69°55′W	5400	5447	2.11	(34.9)	NADW-(AABW)	−33 ± 13	(−2.0)	(−79 ± 13)	125
6/15/55	25°07′N	69°57′W	5508	5564	(2.2)	34.74	NADW-(AABW)	−53 ± 20	(−2.0)	(−99 ± 20)	127
4/16/56	25°01′N	59°12′W	6035	6081	(2.0)	(34.9)	NADW-(AABW)	−88 ± 6	−7.3	−124 ± 6	128
10/11/56	24°23′N	24°03′W	4921	5104	(2.5)	34.92	NADW (E. Basin)	−82 ± 5	+1.5	−135 ± 5	129
6/20/55	24°05′N	68°23′W	5584	5649	(2.2)	(34.9)	NADW-(AABW)	−58 ± 8	(−2.0)	(−104 ± 8)	130
6/17/55	23°28′N	65°56′W	5788	5835	(2.5)	34.76	NADW-(AABW)	−55 ± 13	(−2.0)	(−101 ± 13)	131
4/14/56	22°22′N	54°19′W	5608	5654	(2.0)	(34.9)	NADW-(AABW)	−87 ± 6	−6.6	−125 ± 6	132
12/31/56	15°52′N	38°08′W	5264	5300	(2.4)	34.86	NADW (E. Basin)	−65 ± 7	+2.3	−119 ± 7	133
11/26/57	15°29′N	40°30′W	4147	4330	2.45	34.67	NADW (E. Basin)	−83 ± 9	−4.0	−126 ± 9	134
2/16/56	03°26′S	31°34′W	4389	4429	(0.8)	(34.80)	AABW	−99 ± 7	+0.6	−150 ± 7	135
1/22/57	16°34′S	28°03′W	5330	5376	(0.5)	34.69	AABW	−105 ± 6	−2.5	−150 ± 6	136
2/ 1/57	33°43′S	45°18′W	4380	4426	(0.0)	(34.7)	AABW	−88 ± 5	−3.3	−132 ± 5	137

* Values listed in parentheses were estimated from published oceanographic data for the location and depth of the sample. Direct measurements are not available.

† See text for definition of abbreviations.

‡ δC¹³ values are estimated rather than measured. The corresponding ΔC¹⁴ values are based on these estimates.

southern latitudes and gradually becoming warmer and more saline as it mixes with overlying water and moves northward. Traces of this water, highly diluted, can be observed as far as 35°N in the western North Atlantic. Because this water mass lies along the ocean bottom its thickness is highly variable, depending upon the bottom topography. Its upper limits extend to about 3600 meters at 40°S, dropping to 4500 meters at 25°N. Small amounts of AABW are believed to enter the eastern Atlantic basin through deep gaps in the Mid-Atlantic Ridge located at the equator and at 10°N.

North Atlantic Deep Water (NADW). This water mass is the most extensive in the Atlantic and is thought to form at the surface in the region of southern Greenland. In this area cool waters from the north mix with Atlantic surface water of higher salinity to form a mixture having a temperature of approximately 2.5°C and a salinity of 34.9 per mil. This water sinks and moves southward to occupy the depths between 1500 and 4000 meters throughout the Atlantic, extending nearly to the Antarctic region.

The samples included in the present survey were collected as nearly as possible from regions where useful correlations with present water-mass concepts could be made. Where possible, independent hydrographic measurements were made to establish a firm relationship between the water sampled with the large-volume sampler and the water masses in the area. In three cases where depth control is considered inadequate, the results have not been used. The measurements presented apply to samples that have a maximum estimated depth error of ±50 meters. This depth uncertainty is in no way critical to the conclusions based on these data.

The locations of the surface water samples measured as part of this study are shown in Figure 2. The first number beside each sample location is the chart index number from Table 1 and the second number indicates the ΔC^{14} value. Major currents together with directional arrows are shown in a highly generalized fashion.

The most striking feature in the pattern of surface sample results is the systematic change from lower to higher C^{14}/C^{12} ratios in the samples taken from the Antarctic northward. The effect appears to continue farther north than is indicated by the samples on this chart, the results of *Fonselius and 'Ostlund* [1959] for samples from between 60° and 80°N averaging −35 per mil.

The one sample (No. 51) taken south of the Antarctic Convergence yielded the lowest C^{14}/C^{12} ratio of all surface samples. This finding is consistent with that of *Burling and Garner* [in press], who report that the lowest surface C^{14} activities were found in samples from south of the Antarctic Convergence in the region adjacent to New Zealand. The explanation here is the same as that for the South Pacific samples. Deep water which rises to the surface in the circumpolar region south of the Antarctic Convergence is returned to depth before its C^{14} content can reach equilibrium with the atmosphere.

The average ΔC^{14} value for 16 South Atlantic surface samples (excluding the Antarctic and Falkland Current samples) is −57 per mil. Although variations exist they show no systematic pattern. The Falkland Current appears to bring water of low C^{14}/C^{12} ratio northward from the Drake Passage. The southward-flowing Brazil Current water has a considerably higher C^{14}/C^{12} ratio. Where the two meet and move eastward as the Brazil Current Extension the C^{14} content appears to have an intermediate value. It is tempting to assign some significance to the apparent lowering of the surface C^{14} values from west to east across the Benguela Current in the region near South Africa. It is known that extensive upwelling of deeper water occurs on the coastal side of the current. Whereas the radiocarbon data are consistent with this circulation pattern the samples are too few and the differences too small to justify any independent conclusions.

The average of 18 samples from the surface North Atlantic is −49 per mil, a difference of 8 per mil from the South Atlantic surface water average. The Caribbean has a value (based on ten measurements) intermediate between the two. This is to be expected, since it receives water from both North and South Atlantic mixed layers. Among the samples shown for the North Atlantic there is no apparent correlation of ΔC^{14} values with local hydrographic features.

The locations of subsurface samples measured as part of this study are shown in Figure 3.

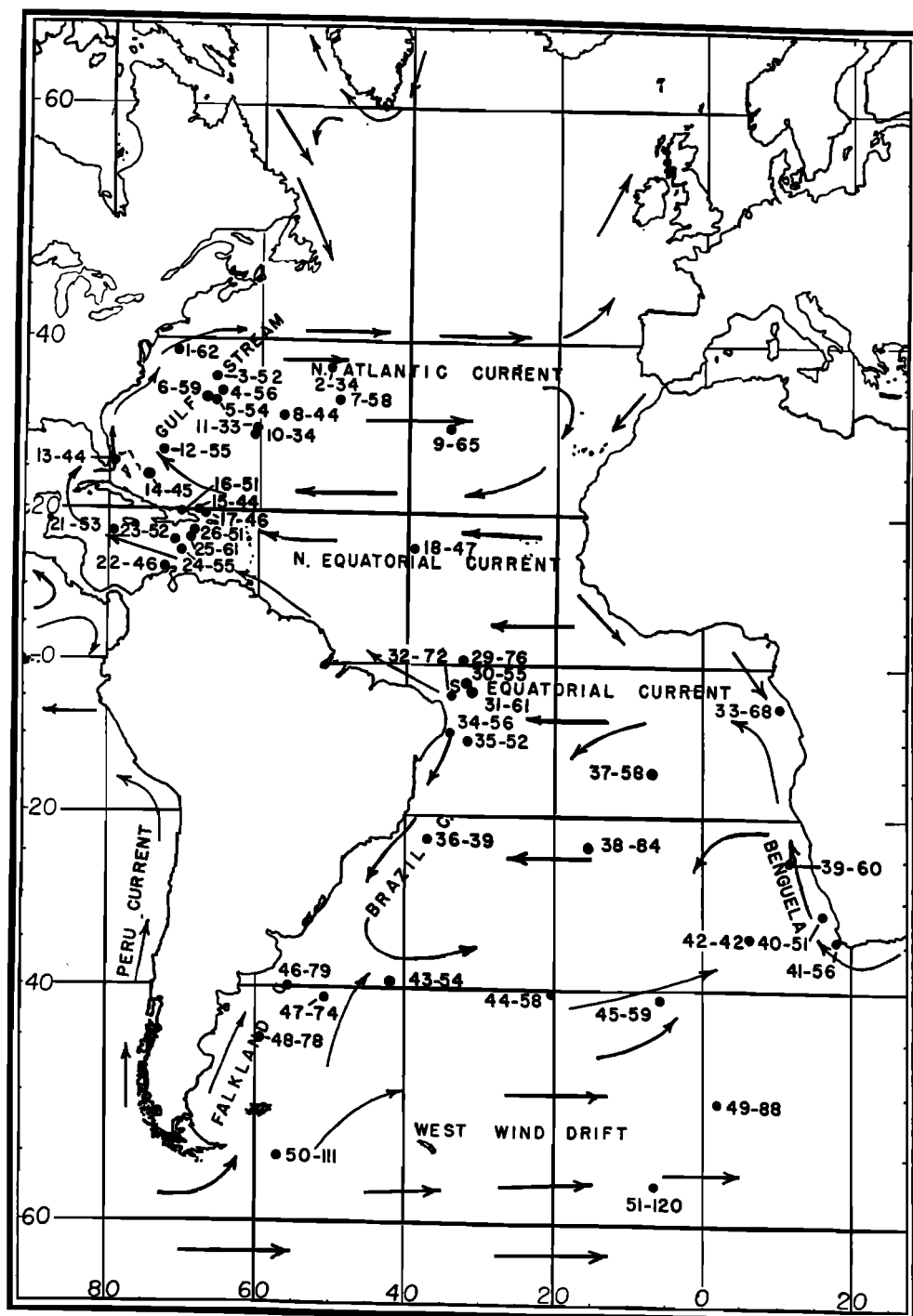Fig. 2. Locations of surface water samples. The first number beside each dot is the index number and the second the ΔC^{14} value. The arrows show the pattern of surface water movement.
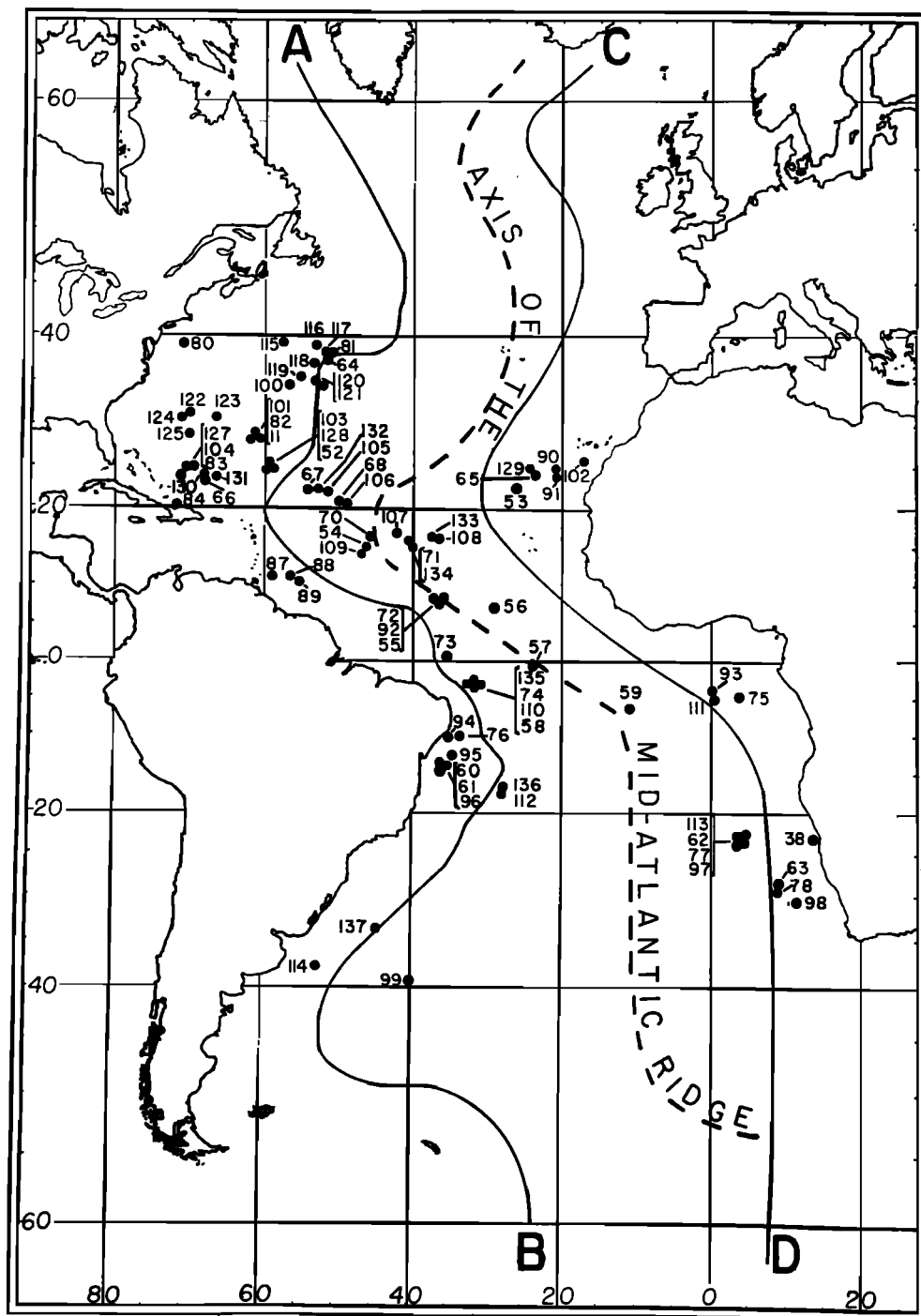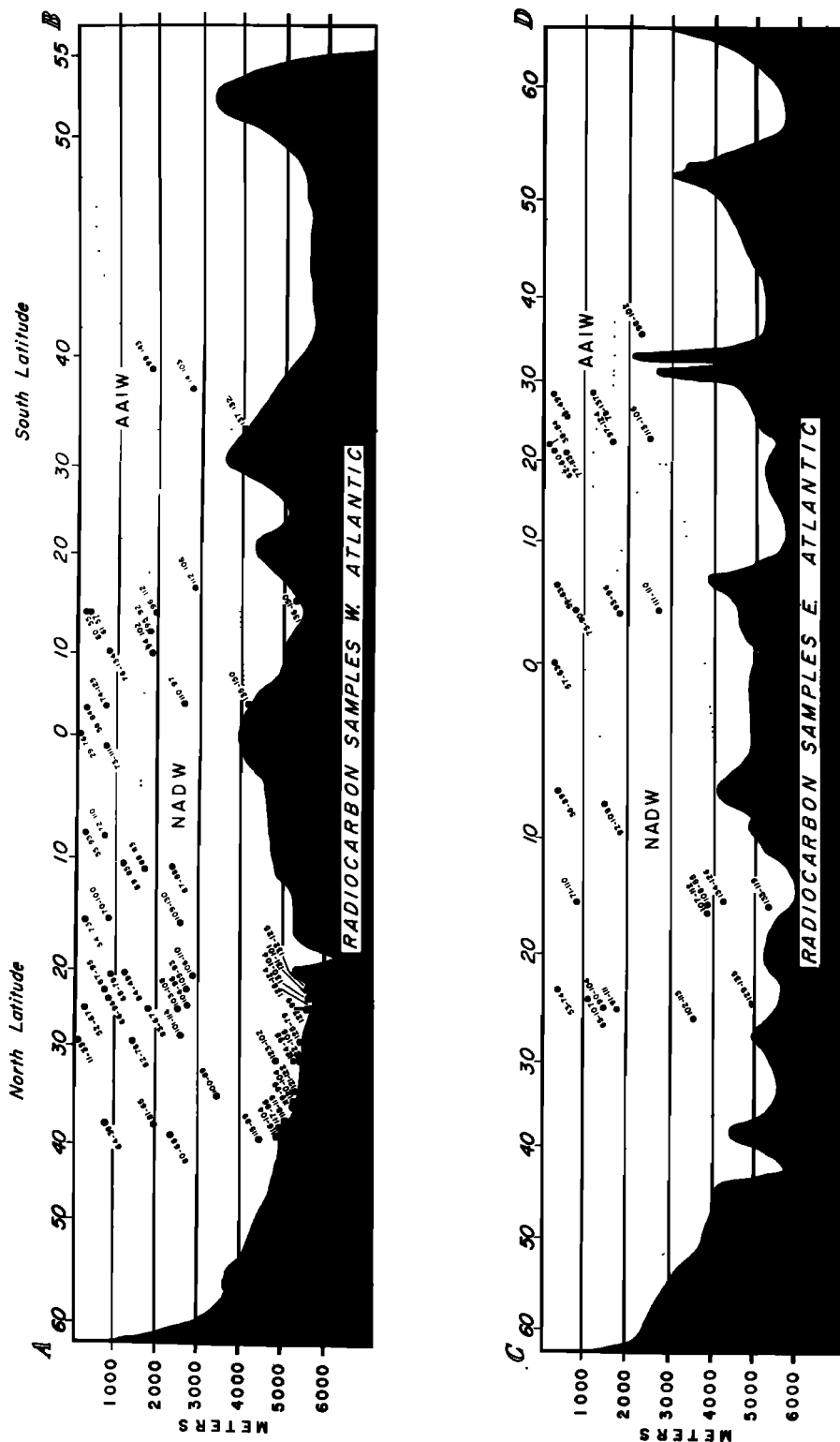
Fig. 3. Locations of subsurface water samples. The number beside each dot is the index number given in Table 1. The lines *A–B* and *C–D* give the location of the depth profiles shown in Figure 4.

Fig. 4. Locations of subsurface ocean water samples projected onto north-south profiles through the western basin (upper) and eastern basin (lower) of the Atlantic Ocean. The first number beside each dot is the sample index number and the second the ΔC^{14} value. The location of the profiles is given in Figure 3.

Their depth distribution is illustrated on two longitudinal cross sections in Figure 4; one drawn through the eastern and one through the western trough of the Atlantic Ocean. Table 5 gives average ΔC^{14} values for the results from the various types of water.

In the North Atlantic between 15° and 30°N and at a depth between 200 and 400 meters three measurements were made, the C^{14} values averaging −71 per mil. This average, which should be representative of the NACW, is significantly lower than that for the overlying surface water and higher than that for the underlying water.

Eight samples in the North Atlantic from a depth of 800 to 1100 meters average −99 per mil. These samples probably consist of a mixture of AAIW with water of higher temperature and salinity from the North Atlantic and the Mediterranean, the percentage of the latter two increasing northward. Such a distribution is supported by the C^{14} values which show a northward increase in C^{14}/C^{12} ratio. At this same level at 38°N a much higher C^{14}/C^{12} ratio was obtained (sample 64, $\Delta C^{14} = -39$ per mil), which suggests not only that the AAIW has ceased to be an influence but also that water which might be defined as Arctic Intermediate Water is present.

In the western Atlantic between 10° and 40°N and from 1200 to 2400 meters in depth the C^{14} average for a group of eight samples is −72 per mil. This group appears to represent a C^{14} maximum level, perhaps being fed by eddy currents emanating from the western boundary current. [*Wüst*, 1935; *Stommel*, 1958; *Swallow and Worthington*, 1957].

In the eastern North Atlantic and in the equatorial region of the western Atlantic, samples from the same depth as the maximum C^{14} layer yield C^{14}/C^{12} ratios identical with those of the North Atlantic Deep Water. It is possible that these areas lie beyond the influence of the boundary current.

Fifteen samples from the core of the NADW in both basins average −105 per mil. No trend with latitude is apparent. Whereas the values for the lower Deep Water in the western trough agree with those for the overlying core water, the lower Deep Water in the eastern trough has a 27 per mil lower average than the average for

the overlying water. Although this difference suggests a longer residence time for water in the eastern basin, it is possible that it represents, at least in part, contamination by water of Antarctic origin.

The South Atlantic samples corresponding to the Central Water mass (57, 58, 60 to 63) have C^{14}/C^{12} ratios about 10 per mil higher than the corresponding NACW and 5 per mil lower than the overlying surface water.

The Antarctic Intermediate Water in the South Atlantic is characterized by a relatively low C^{14}/C^{12} ratio. Six samples between the equator and 40°S average −118 per mil.

Samples from 20° to 40°S (97 to 99) at depths between 1500 and 2200 meters show a significantly lower C^{14}/C^{12} ratio than is found farther north at similar depths. Because of the significantly lower salinities, this appears to be the result of mixing with lower-activity Antarctic water rather than of a longer residence time.

Antarctic Bottom Water of nearly pure type has been sampled in three places (135 to 137) in the southwestern Atlantic. Its average C^{14} value of −144 per mil is the lowest found thus far in the Atlantic Ocean.

The radiocarbon results on a total of 78 subsurface samples from the Atlantic suggest that samples taken within the core of a single water mass (as defined in oceanographic terms) show a standard deviation in ΔC^{14} value only slightly exceeding the measurement error. Since significant differences exist between the various masses, it would appear that circulation within a water mass is relatively rapid with respect to the residence time of water particles in the mass.

Discussion. In order to obtain absolute mixing rate estimates from the radiocarbon data a model of the operation of the oceans must be set up on the basis of existing oceanographic data. The resulting rates will be only as good as the model. In order to demonstrate the importance of the type of model adopted, two quite different sets of assumptions will be examined. In the first case the oceans are assumed to be at steady state (that is, the temperature, salinity, C^{14}/C^{12} ratio, etc., for any point in the ocean remains constant with time). The second model involves periods of rapid oceanic mixing separated in time by periods during which mix-
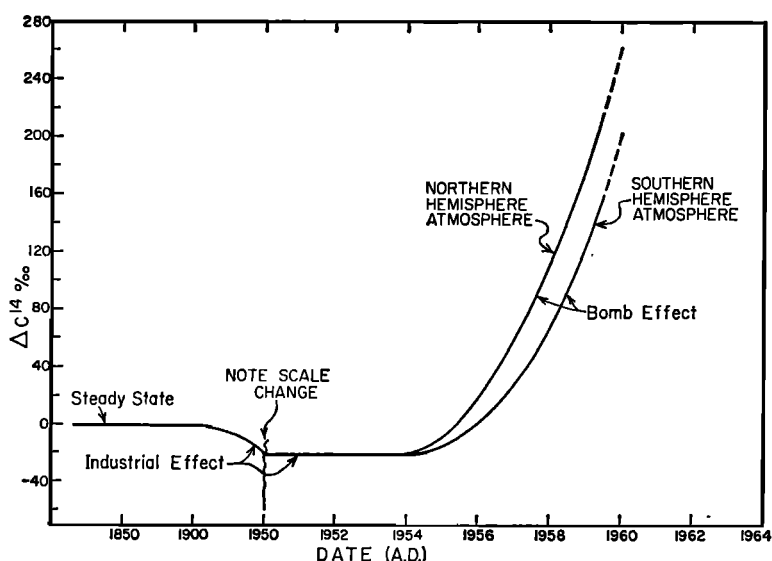
Fig. 5. Variation in the ΔC^{14} value for atmospheric CO_2 over the last century. The decrease beginning in about 1900 is the result of the addition of industrial CO_2, and the rise beginning in 1954 is the result of C^{14} produced during nuclear tests.

ing is greatly restricted. In this case the properties characterizing any unit of volume in the ocean will change with time.

Steady-state models. Numerous investigators have shown that the C^{14} concentration in the atmosphere and surface water is presently not at steady state as the result of industrial CO_2 and bomb-produced C^{14}. If calculations based on steady-state assumptions are to be made, it is necessary to determine what the concentrations of C^{14} in the samples measured would have been if the system had not been contaminated.

The correction for bomb-produced C^{14} is accomplished as follows. Measurements of the C^{14} concentration in atmospheric CO_2 and in vegetation define the rise in the C^{14}/C^{12} ratio for the tropospheric reservoir (see Fig. 5). Using the steady-state model described below it is possible by successive approximation to estimate how much bomb-produced C^{14} was present in surface ocean water at any given time. Such calculations indicate that samples collected before 1956 should contain negligible bomb-produced C^{14}. The results for such samples are given in Table 2, column 3, averaged on a geographical basis. A correction based on the model calculation has been made for each sample collected after 1956. The corrected averages for these samples are

given in column 4. Estimates of the prebomb concentrations based on results from samples taken both before and after January 1, 1956, are given in column 5. The C^{14} results of *Rafter and Fergusson* [1958] for the western South Pacific surface water and of *Fonselius and Ostlund* [1959] for the northern North Atlantic surface water have been treated in the same manner and are included for reference. These results should be strictly comparable, since interlaboratory calibrations have been carried out in each case (Table 3). Since the differences between the corrected (column 5) and uncorrected (column 2) averages are in all cases less than 1 per cent, the uncertainty in the corrections introduces no significant error into the calculations which follow. No correction has been made for samples from the deep water masses, as the model indicates that the amount of bomb-produced C^{14} added to these reservoirs would be negligible compared with that already present. For a more complete discussion of the quantity and distribution of bomb-produced C^{14} see *Broecker and Walton* [1959a] and *Broecker and Olson* [in press].

Suess [1955], *Hayes, Anderson, and Arnold* [1955], *Brannon, Daughtry, Perry, Whitaker, and Williams* [1957], *Fergusson* [1958], and

TABLE 2. Correction for Bomb-Produced Radiocarbon†† in Surface Ocean Water

Geographic Region	Uncorrected Avg.				Avg. pre-1/1/56 Samples§				Avg. post-1/1/56 Samples‖				Corrected Avg.			
	Avg.	No.	S.D.¶	S.E.**	Avg.	No.	S.D.¶	S.E.**	Avg.	No.	S.D.¶	S.E.**	Avg.	No.	S.D.¶	S.E.**
North Atlantic† 60°–80°N	−35	3	±2	±4	...	0	...	...	−38	3	±2	±4	−38	3	±2	±4
North Atlantic* 15°–40°N	−49	18	±10	±3	−49	9	±8	±3	−54	9	±9	±3	−52	18	±9	±2
Caribbean*	−56	8	±9	±3	−56	8	±9	±3	...	0	...	...	−56	8	±9	±3
South Atlantic* 0°–40°S	−57	16	±10	±3	...	0	...	...	−63	16	±10	±3	−63	16	±10	±3
Falkland Current	−77	3	±3	±4	...	0	...	...	−80	3	±3	±4	−80	3	±3	±4
Antarctic†* (temp. <3°C)	−120	3	±10	±6	...	0	...	...	−123	3	±10	±6	−123	3	±10	±6
South Pacific† 15°–42°S	−41	16	±8	±2	−54	2	±2	±3	−48	14	±6	±2	−49	16	±6	±2

* Based on results given in this paper.
† Based on results published by *Rafter and Fergusson* [1958].
‡ Based on results published by *Fonselius and Ostlund* [1959].
§ Uncorrected (bomb-produced C^{14} assumed negligible).
‖ Corrected for bomb-produced C^{14} using steady-state circulation model.
¶ Standard deviation of results from mean.
** Standard error on the mean (based on the larger of the S.D. or average laboratory error).
†† All results given in ΔC^{14} units (‰).

TABLE 3. Interlaboratory Calibration (The results are given on the ΔC^{14} scale as per mil difference from 0.950 the activity of the N.B.S. oxalic acid reference standard used as a primary standard by all three laboratories.)*

	Lamont	New Zealand	Stockholm
Lamont wood standard (1890 oak)	-6 ± 5†	...	...
New Zealand wood standard (contemporary pine)	-18 ± 6	-20 ± 4	...
Stockholm wood standard (1850 oak)	8 ± 6	...	6 ± 5

* The following relationships have been used to convert the data on ocean water samples given by *Rafter and Fergusson* [1958] and *Fonselius and Ostlund* [1959] to the ΔC^{14} scale.

$$\Delta C^{14} = 10R + 6.0 \quad \text{(Stockholm results)}$$

$$\Delta C^{14} = 10 \left[\begin{array}{c} \% \ C^{14} \ \text{enrichment} \\ \text{W.R.T. N.Z. wood} \\ \text{standard} \end{array} \right] - 66.0$$

$$\text{(New Zealand results)}$$

† This result supersedes that of 0 ± 5 published by *Broecker and Olson* [1959]. The change is the result of further comparison measurements.

Munnich and Vogel [1958] have published data relating to the decrease in the atmospheric C^{14}/C^{12} ratio as the result of the consumption of fossil fuels. The combined results suggest a 25 ± 10 per mil reduction in the average atmospheric C^{14}/C^{12} ratio between 1855 and 1955. Measurements of comparable accuracy are not available for the surface oceans. Again the steady-state model discussed below has been used to estimate the magnitude of the oceanic reduction. Such calculations suggest that the reduction in the C^{14}/C^{12} ratio in the surface 100 meters of the Atlantic and Pacific oceans should be 0.67 of that for the atmosphere. A value of $0.40 \pm .20$ of the atmospheric reduction is estimated for the vertically mixed regions at the northern and southern extremes of the ocean. The preindustrial-revolution ΔC^{14} values estimated for various areas on this basis are listed in Table 4. Assuming that the entire surface of the Pacific and Indian Oceans has ΔC^{14} values averaging close to those of *Rafter and Fergusson* [1958]

for the southwestern Pacific, a world-average ΔC^{14} value has been computed for surface ocean water in 1955 and in 1855. Again, for the deep water masses the reduction in the C^{14}/C^{12} ratio as a result of equilibration with 'fossil' CO_2 can be considered negligible in most cases.

Estimates of the mean residence times of water molecules in the subsurface water masses of the Atlantic Ocean can easily be made if the following assumptions are valid: (1) circulation in the oceans is at steady state; (2) the corrected ΔC^{14} value for surface water in the convergence (the area considered on the basis of oceanographic evidence to be the source region for a given subsurface water mass) characterizes the 'new' water continually being added to the mass; (3) mixing between adjacent subsurface water masses does not measurably alter their respective C^{14}/C^{12} ratios; (4) CO_2 supplied to a subsurface mass through solution of carbonate sediment and through the oxidation of organic material does not measurably alter the C^{14}/C^{12} ratio of the CO_2 initially present in the mass. In this case, in the age range of 0 to 1000 years,

$$\tau_M = 8.04 \left[(\Delta C^{14}_{surface} - \Delta C^{14}_{depth}) - \frac{(\Delta C^{14^2}_{surface} - \Delta C^{14^2}_{depth})}{2000} \right] \text{yr}$$

where τ_M is the mean residence time of H_2O molecules within a given water mass (in other words, the time required for a volume of water equal to that contained in the deep water mass to be supplied from the surface source region).

The results of computations made on this basis for the various subsurface water masses of the Atlantic Ocean are given in Table 5. The locations of the source areas for the individual water masses are those given in *Sverdrup, Johnson, and Fleming* [1942]. The errors quoted are based on the uncertainty in the measurement averages only and hence do not include the uncertainty in the assumptions upon which the calculations are based.

The results suggest the following conclusions:

1. Water masses originating in the Antarctic are in general characterized by shorter residence times than those originating in the high latitudes of the North Atlantic.

TABLE 4. Correction for Industrial CO_2 Effect in Surface Oceans

Geographic Location	Average ΔC^{14} Surface Oceans 1955 (see Table 2), ‰	Fraction Atmospheric Industrial CO_2 Effect (based on model calculations)	Estimated ΔC^{14} Reduction from Industrial CO_2* (1855 to 1955), ‰	Average ΔC^{14} Surface Oceans 1855 (calculated), ‰
North Atlantic 60°–80°N	−38 ± 4	.40 ± .20	10 ± 8	−28 ± 9
North Atlantic 15°–40°N	−52 ± 2	.67 ± .15	17 ± 7	−35 ± 7
Caribbean Sea	−56 ± 3	.67 ± .15	17 ± 7	−39 ± 8
South Atlantic 0°–40°S	−63 ± 3	.67 ± .15	17 ± 7	−46 ± 8
Falkland Current	−80 ± 4	.40 ± .15	10 ± 8	−70 ± 9
Antarctic <3°C	−123 ± 6	.40 ± .25	10 ± 8	−113 ± 10
South Pacific 15°–42°S	−49 ± 2	.67 ± .15	17 ± 7	−32 ± 7
Average surface ocean	−58 ± 10	.60 ± .15	15 ± 8	−43 ± 13

* Assumes industrial CO_2 effect in atmosphere of −25 ± 10 per mil in 1955.

2. Except for the NACW and for the wedge of water lying at depths between 1200 and 2400 meters in the western North Atlantic, most of the subsurface water of North Atlantic origin appears to be at least 600 years 'old.'

3. Whereas the deepest waters in the western basin of the North Atlantic have the same residence time as the overlying water, the water below 4000 meters in the eastern basin appears to have a significantly higher residence time (900 years as opposed to ~ 650 years).

4. Samples from the SACW appear to have ΔC^{14} values nearly identical to those for surface water samples taken in the outcrop area of the water mass. This suggests that the water is in fairly rapid communication with the surface. The decrease in ΔC^{14} toward the bottom of the mass may be the result of mixing with the low-C^{14} water of the AAIW mass either at depth or in the outcrop region. In this case, the added uncertainty in the relative correction for the industrial effect for the surface and subsurface masses becomes important, yielding a possible range of apparent ages from 0 to 200 years.

Of the four assumptions on which these residence times are based only the fourth can be adequately verified. The amount of CO_2 added to the subsurface water masses of the Atlantic through oxidation of organic material does not exceed 10 per cent of the CO_2 initially present. If the oxidized organic material were carried along with the surface water entering the mass, it would probably have the same ΔC^{14} value as the water and hence would have no effect. If, on the other hand, the organic material settled downward rapidly from the surface water, the CO_2 produced by oxidation would have a ΔC^{14} value significantly higher than that of the deep water to which it was added—as much as 30 per mil in the North Atlantic and 80 per mil in the South Atlantic, assuming that oxygen is being consumed at a linear rate. The maximum for the South Atlantic exceeds that for the North Atlantic because of the shorter residence times and the greater surface-depth contrast in ΔC^{14} in the South Atlantic. Thus for the worst case (that is, if all the organic material oxidized in a deep water mass has the ΔC^{14} of the overlying surface water), the residence times quoted would have to be increased by 30 years in the North Atlantic and 70 years in the South Atlantic.

The steady-state rate at which carbonate sediments would have to be dissolved and/or exchanged in order measurably to alter the C^{14}/C^{13} ratio in near-bottom water masses is prohibitively large, exceeding the average rate of

TABLE 5.   Mean Residence Time Estimates for Subsurface Water Masses of the Atlantic Ocean (subject to validity of assumptions stated in text)

| Location and Depth | C¹⁴ Results on Samples from within Mass | | | | Index No. of Samples Used in Calculation of Averages | Estimated Pre-Industrial Revolution ΔC^{14} Value for Source Area, ‰ | M, years |
	Average ΔC^{14}, ‰	No.	S.D., ‰	S.E., ‰			
North Atlantic 15°–30°N, 200–400 m	−71	3	±4	±4	52–54	−35 ± 7	300 ± 70
North Atlantic 5°–25°N, 800–1100 m	−99	8	±11	±4	65–72	−28 ± 9	640 ± 90
Western North Atlantic 10°–40°N, 1200–2400 m	−72	8	±16	±6	80–84, 87–89	−28 ± 9	380 ± 100
Central Atlantic 0°–40°W, 20°S–25°N, 1400–2000 m	−104	7	±8	±3	90–96	−28 ± 9	690 ± 90
North Atlantic Deep Water 40°S–35°N, 2500–4000 m	−105	15	±11	±3	100–114	−28 ± 9	700 ± 90*
North Atlantic Bottom Water 23°–40°N, Western Basin, >4000 m	−104 (−100)†	16	±13	±3	115–127, 130, 131	−28 ± 9	690 ± 90
North Atlantic Bottom Water 15°–25°N, Eastern Basin, >4000 m	−127 (−123)†	3	±8	±5	129, 133, 134	−28 ± 9	920 ± 100
South Atlantic 30°–0°S, 200–400 m	−61	6	±12	±5	57, 58, 60–63	−46 ± 8	<250
South Atlantic 40°–0°S, 500–1200 m	−118	6	±17	±7	73–78	−90 ± 20	<350*
South Atlantic 40°S–20°S, 1500–2200 m	−130	3	±12	±7	97–99	. . .	. . .
Antarctic Bottom Water 35°–0°S, >4000 m	−144	3	±10	±6	135–137	−113 ± 15	<350*

* These averages represent the cores of well-defined water masses; NADW, AAIW, and AABW.
† Corrected for the contribution of AABW (based on estimates given by *Wüst*, 1957b).

accumulation of carbonate oozes. Deep sea cores show no evidence of large-scale carbonate solution, and the possibility of sufficiently rapid exchange between the carbonates in the sediments and the overlying water is excluded by the fact that the C¹⁴-age and O¹⁸-temperature records are preserved in deep sea carbonates. From these and numerous other lines of evidence it can be shown that the presence of carbonate sediments cannot measurably influence the residence time computed for the overlying water mass. In red clay areas carbonate falling from the surface is presumably redissolved before or soon after reaching the bottom. In this case the CO_2 added to the water through carbonate solution may well be higher in C¹⁴ than the water itself. Using an addition rate comparable to the sedimentation rate of carbonate in globigerina ooze areas (~ 1 g/cm²/1000 yr) and assuming that the dissolved carbonate is mixed throughout the lower 100 meters of ocean water, the addition per 100 years would be equivalent to 5.0 per cent of the total CO_2 already present in the water. If this is the case the contribution to the apparent age of the water from this source is negligible.
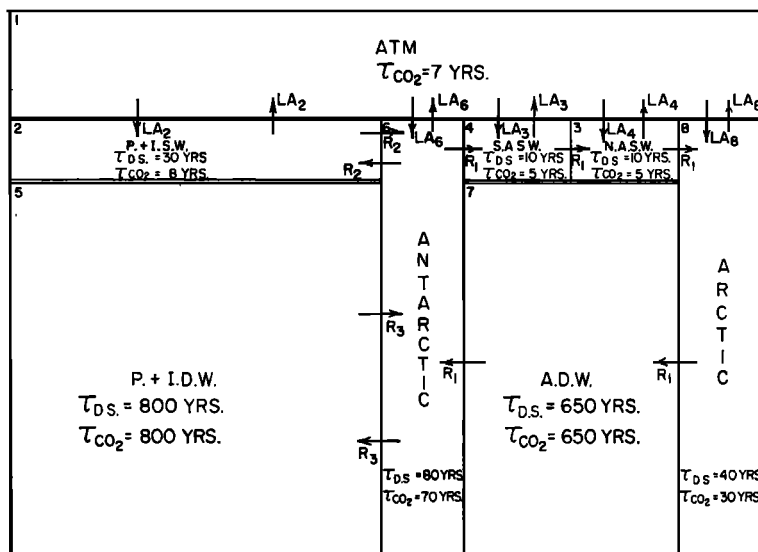
ATM
τ_{CO_2}=7 YRS.

LA₂ ... LA₆ ... LA₃ ... LA₄ ... LA₈

2 LA₂
P.+I.S.W.
$\tau_{D.S.}$ = 30 YRS
τ_{CO_2} = 8 YRS.
R₂

6 LA₆ R₂

4 LA₃
S.A.S.W.
$\tau_{D.S.}$ =10 YRS
τ_{CO_2} = 5 YRS.
R₁

3 LA₄
N.A.S.W.
$\tau_{D.S.}$ =10 YRS
τ_{CO_2} = 5 YRS.
R₁

8 LA₈ R₁

5

7

ANTARCTIC

ARCTIC

P. + I.D.W.
$\tau_{D.S.}$ = 800 YRS.
τ_{CO_2}= 800 YRS.

A.D.W.
$\tau_{D.S.}$ = 650 YRS.
τ_{CO_2} = 650 YRS.

R₃   R₁

$\tau_{D.S.}$ =80 YRS
τ_{CO_2}=70 YRS

$\tau_{D.S.}$ =40 YRS.
τ_{CO_2} =30 YRS

Fig. 6. Model of steady-state CO_2 cycle in the atmosphere and oceans. The numbers in the upper left-hand corner of each box identify the reservoir. The arrows indicate possible modes of transfer between reservoirs, and the letters show the rates of transfer. The CO_2 and DS (dissolved solid) mean residence times differ because significant quantities of CO_2 are transferred through the atmosphere.

In the case of the samples from the cores of the NADW, AAIW, and AABW, complications resulting from mixing at depth are at a minimum. For the other entries in Table 5 the possible effects of mixing must be considered. For example, in the case of the central water systems, where vertical temperature gradients suggest mixing of water of more than one source, it is possible that ages computed in the above manner are in error. Thus, as suggested by *Bowen and Sugihara* [1960], the 300 year age computed for the NACW may be too great. The low ΔC^{14} value could, as they propose, be the result of mixing with the underlying low ΔC^{14} NADW mass. Certainly the natural radiocarbon method is more valuable in the study of deep water masses than in the study of near-surface masses where mixing is serious and where natural radioactive tracers of shorter half-life or man-made radioactive tracers may be used.

Mixing between the NADW and the AABW poses a problem when bottom water samples from the Atlantic are analyzed. From potential temperature and salinity data *Wüst* [1957b] estimated the relative proportions of each type of water at various locations in the Atlantic. Using Wüst's estimates the results for bottom

samples primarily of North Atlantic origin have been corrected for the decrease in C^{14}/C^{12} ratio introduced by the admixture of AABW. These corrections range from 2 to 5 per mil with one (index No. 128) as high as 8 per mil. As shown in Table 5, correction for the contribution of AABW changes the bottom water averages in both basins by only 4 per mil.

The validity of the second as well as the first assumption depends on how close the ocean is to steady-state circulation. Discussion of this point will be deferred to a later section of this paper.

If the ocean is at steady state it should be possible to construct a circulation model consistent with oceanographic evidence which will yield the observed distribution of C^{14} in the ocean-atmosphere system. Such models have been discussed by *Arnold and Anderson* [1957], *Suess and Revelle* [1957], *Craig* [1957a], *Brannon, Daughtry, Perry, Whitaker, and Williams* [1957]. The present model is designed to incorporate more details of the system than could be handled by the three-layer (atmosphere, surface ocean, deep ocean) models used by the above authors without greatly increasing the number of unknown parameters. As is shown in

TABLE 6. Parameters Defining Reservoirs for Steady-State Ocean-Atmosphere Model

Reservoir No.	Reservoir Name	Latitude Range	Depth Range, meters	Surface Area, meter²	CO_2 Content, moles	ΔC^{14}, ‰
1	Atmosphere	Entire	Entire	360×10^{12}	57×10^{15}	0
2	Pacific + Indian Surface Water	<50°S	<100	220×10^{12}	50×10^{15}	−32
3	South Atlantic Surface Water	50°S–5°N	<100	40×10^{12}	9×10^{15}	...
4	North Atlantic Surface Water	5°N–55°N	<100	40×10^{12}	9×10^{15}	−35
5	Pacific + Indian Deep Water	<50°S	>100	...	1980×10^{15}	−200*
6	Antarctic	>50°S	Entire	45×10^{12}	420×10^{15}	...
7	Atlantic Deep Water	50°S–55°N	>100	...	655×10^{15}	−104
8	Arctic	>55°N	Entire	15×10^{12}	40×10^{15}	...
T	Reservoirs 2-8	Entire	Entire	360×10^{12}	3220×10^{15}	−160

* Based on results given by *Rafter and Fergusson* [1958], and *Suess, Rakestraw, and Oeschger* [1959] and on two results obtained at Lamont on deep water samples collected by the University of Washington south of the Aleutians ($\Delta C^{14} = -233 \pm 7$ and -210 ± 9).

Figure 6, the ocean has been divided into seven internally homogeneous reservoirs. Mixing between the reservoirs proceeds only as is indicated by the arrows. The Atlantic Ocean is characterized by a northward transfer of surface water from the Antarctic to the South Atlantic to the North Atlantic to the Arctic, balanced by a return flow from the Arctic to the Antarctic through the NADW system. The Atlantic deep water masses of Antarctic origin are considered to be part of the Antarctic reservoir. Because only limited data are available for the Pacific and Indian oceans a simple two-fold division has been made—one surface and one deep water reservoir. Mixing across the main thermocline in the North and South Atlantic and Pacific-Indian surface reservoirs is assumed to be negligible, the deep water masses being fed from vertically mixed reservoirs at the extremes of the ocean. Transfer from the Pacific to the Arctic reservoir through the Bering Strait is assumed to be negligible. Transfer of CO_2 from the ocean to the atmosphere is assumed to occur at a uniform rate everywhere. The locations and depth ranges are tabulated for each reservoir (Table 6).

At steady state the ΔC^{14} values for the various reservoirs are governed by the following equations:

$$L A_1 \left(\frac{\Delta C^{14}_1 - \Delta C^{14}_{ASW}}{1000} \right) = \lambda (T_2 + T_3$$

$$+ T_4 + T_5 + T_6 + T_7 + T_8)$$

$$\times \left(1 + \frac{\Delta C^{14}_T}{1000} \right) \quad \text{Reservoir 1}$$

$$L A_2 \left(\frac{\Delta C^{14}_1 - \Delta C^{14}_2}{1000} \right) + R_2 \left(\frac{\Delta C^{14}_6 - \Delta C^{14}_2}{1000} \right)$$

$$= T_2 \lambda \left(1 + \frac{\Delta C^{14}_2}{1000} \right) \quad \text{Reservoir 2}$$

$$L A_3 \left(\frac{\Delta C^{14}_1 - \Delta C^{14}_3}{1000} \right) + R_1 \left(\frac{\Delta C^{14}_6 - \Delta C^{14}_3}{1000} \right)$$

$$= T_3 \lambda \left(1 + \frac{\Delta C^{14}_3}{1000} \right) \quad \text{Reservoir 3}$$

$$L A_4 \left(\frac{\Delta C^{14}_1 - \Delta C^{14}_4}{1000} \right) + R_1 \left(\frac{\Delta C^{14}_3 - \Delta C^{14}_4}{1000} \right)$$

$$= T_4 \lambda \left(1 + \frac{\Delta C^{14}_4}{1000} \right) \quad \text{Reservoir 4}$$

$$R_3 \left(\frac{\Delta C^{14}_6 - \Delta C^{14}_5}{1000} \right)$$

$$= T_5 \lambda \left(1 + \frac{\Delta C^{14}_5}{1000} \right) \quad \text{Reservoir 5}$$

$$LA_6\left(\frac{\Delta C^{14}_1 - \Delta C^{14}_6}{1000}\right) + R_2\left(\frac{\Delta C^{14}_2 - \Delta C^{14}_6}{1000}\right)$$

$$+ R_3\left(\frac{\Delta C^{14}_5 - \Delta C^{14}_6}{1000}\right)$$

$$+ R_1\left(\frac{\Delta C^{14}_7 - \Delta C^{14}_6}{1000}\right)$$

$$= T_6\lambda\left(1 + \frac{\Delta C^{14}_6}{1000}\right) \qquad \text{Reservoir 6}$$

$$R_1\left(\frac{\Delta C^{14}_8 - \Delta C^{14}_7}{1000}\right)$$

$$= T_7\lambda\left(1 + \frac{\Delta C^{14}_7}{1000}\right) \qquad \text{Reservoir 7}$$

$$LA_8\left(\frac{\Delta C^{14}_1 - \Delta C^{14}_8}{1000}\right) + R_1\left(\frac{\Delta C^{14}_4 - \Delta C^{14}_8}{1000}\right)$$

$$= T_8\lambda\left(1 + \frac{\Delta C^{14}_8}{1000}\right) \qquad \text{Reservoir 8}$$

where L is the rate of exchange of CO_2 between the atmosphere and surface ocean (in moles CO_2/meter^2/year), A_i is the area a given reservoir exposes to the atmosphere (in meter^2), T_i is

the quantity of CO_2 contained in a given reservoir (in moles CO_2), R_i is the rate of transfers of CO_2 from one reservoir to another (in moles CO_2/year), and λ is the decay constant of C^{14} (in years^{-1}).

Of these eight equations seven are linearly independent, allowing seven unknowns to be determined (L, R_1, R_2, R_3, ΔC^{14}_4, ΔC^{14}_6, and ΔC^{14}_8). The values selected for the other parameters appearing in the equation are given in Table 6. The values computed for the unknowns are given in Table 7. The value of L is independent of the arrangement of the reservoirs or the mode of mixing between them. It depends only on the average C^{14}/C^{12} ratio of ocean water, ΔC^{14}_T, and the difference between the average C^{14} concentration in atmospheric and surface ocean CO_2. Since the difference between ΔC^{14}_1 and $\Delta C^{14}_{A sw}$ is known to an accuracy of perhaps 25 per cent and since ΔC^{14}_T is known to an accuracy of about 10 per cent, the estimate of L should be uncertain by no more than 30 per cent. The result confirms similar estimates of this parameter obtained by *Craig* [1957a] and is also in satisfactory agreement with the value of 5 moles/m^2/yr obtained by *Broecker and Walton* [1959b] for four closed basin lakes in the

TABLE 7. Comparison of Results of Steady-State Model Calculations with Independent Estimates

Parameter	Description	Value Based on Model	Independent Estimate	Method
ΔC^{14}_4	C^{14} concentration in South Atlantic Surface Water	$-65 \permil$	$-46 \permil$*	Direct measurement
ΔC^{14}_6	C^{14} concentration in the Antarctic reservoir	$-120 \permil$	$-113 \permil$*	Direct measurement
ΔC^{14}_8	C^{14} concentration in the Arctic reservoir	$-30 \permil$	$-28 \permil$*	Direct measurement
L	Ocean-atmosphere exchange rate	$22 \pm 7 \dfrac{\text{moles } CO_2}{\text{m}^2 \text{ yr}}$	$5 \dfrac{\text{moles } CO_2\dagger}{\text{m}^2 \text{ yr}}$	Inland lakes
R_1	Rate of transfer between reservoirs in Atlantic cycle	$1.0 \times 10^{15} \dfrac{\text{moles } CO_2}{\text{yr}}$	$0.4 \times 10^{15} \dfrac{\text{moles } CO_2\ddagger}{\text{yr}}$	Surface current measurement
R_2	Rate of exchange between P. + I. Surface Water and Antarctic	$1.6 \times 10^{15} \dfrac{\text{moles } CO_2}{\text{yr}}$	$\cdots$	$\cdots$
R_3	Rate of exchange between P. + I. Deep Water and Antarctic	$2.5 \times 10^{15} \dfrac{\text{moles } CO_2}{\text{yr}}$	$\cdots$	$\cdots$

* See Table 4.
† *Broecker and Walton* [1959b] and *Broecker and Olson* [in press].
‡ Based on net northward rate of surface water transport given by *Sverdrup, Johnson, and Fleming* [1942].

Great Basin region of the United States. The latter estimates are based on the steady-state C^{14} concentration in the lake-river systems. Independent confirmation has been obtained in one case (Great Salt Lake) on the basis of the rate of uptake of bomb-produced C^{14} [*Broecker and Olson*, in press]. The higher value for the mean ocean probably reflects a higher degree of surface agitation and hence mixing.

The Δ^{14} values predicted by the model for the Antarctic and Arctic are, as shown in Table 7, in good agreement with estimates based on direct measurements in these areas (see *Fonselius and Ostlund* [1959], *Rafter and Fergusson* [1958], and this paper). The disagreement between the predicted and measured values for the South Atlantic could well indicate back-mixing from the North to the South Atlantic surface system. Agreement could be achieved by superimposing an exchange rate between these reservoirs of about 1.0×10^{15} moles CO_2/yr on the net northward transfer rate of 1.0×10^{15} moles CO_2/yr. Since the one-way mixing cycle adopted for the Atlantic is certainly an over-simplification, a more adequate model would have to take into account back-mixing between each pair of reservoirs. Too many additional parameters are required for any realistic estimates of the magnitude of these effects to be made.

It is of interest to compare net rates of northward transport based on oceanographic data with that of 1.0×10^{15} moles CO_2 per year predicted by the steady-state model. *Sverdrup, Johnson, and Fleming* [1942] gave an estimate equivalent to 0.4×10^{15} moles CO_2 per year for surface currents, and *Wüst* [1957a, 1957b] gave a value equivalent to 0.8×10^{15} moles of CO_2 per year for the upper 200 meters in the South Atlantic.

From these results the mean residence times for both CO_2 and dissolved solids (DS) in the various reservoirs can be computed. The residence times given in Figure 6 are computed by dividing the total amount of CO_2 (or DS) in the reservoir by the rate at which CO_2 (or DS) is being added to the reservoir. It is assumed that atmospheric transfer of dissolved solids is negligible compared with oceanic transport.

Assuming steady state, *Stommel* [1957b] calculated, on the basis of estimates of the quantity of water transported by the Western Boundary Current and by the Antarctic Bottom Water, that the mean residence time for water below 2000 meters should be about 500 years. This estimate agrees favorably with that based on the C^{14} data.

It is of interest to note that, whereas the C^{14}/C^{12} ratio for much of the deep Pacific is about 100 per mil lower than that for the NADW, the

TABLE 8. Comparison of Oceanic Tritium Concentrations Predicted on the Basis of the Steady-State Model with Measured Values*

Reservoir No. (see Fig. 6)	Steady-State Tritium Conc. (predicted if production rate = 0.5T/cm²/sec), T.U.	Steady-State Tritium Conc. (predicted if production rate = 1.5T/cm²/sec), T.U.	Steady-State Tritium Concentration (measured), T.U.
2	0.4	1.1	1.2 (2) S.D. = .4
3	0.2	0.6	...
4	0.3	1.0	1.2 (11) S.D. = .4
5	0.7×10^{-3}	2×10^{-3}	...
6	0.03	0.1	...
7	3×10^{-3}	10×10^{-3}	<0.1 (3)
8	0.1	0.4	...

* Assumes tritium production rate such that between 0.5 and 1.5 tritium atoms/cm²/sec reach the earth's surface (this range includes the estimates made by *Begamann and Libby* [1957] (1.0 T atoms/cm²/sec), *Craig* [1957a] (1.2 ± .5 T atoms/cm²/sec), *Giletti Bazan, and Kulp* [1958] (.75 ± .4 T atoms/cm²/sec), *Bolin* [1958] (.9 ± .2 T atoms/cm²/sec).

† Based on data published by *Giletti* [1958] and by *Begamann and Libby* [1957] (all samples included were collected before March 1954).

computed residence time is only slightly larger. This is true because the source for the deep Pacific has approximately a 90 per mil lower C^{14}/C^{12} ratio than that for the NADW.

One potential test (first suggested by *Craig* [1957*b*]) is to determine whether the distribution of natural tritium in the oceans is consistent with the rates of mixing fixed by the C^{14} distribution. Because no wide coverage of the tritium concentration in the ocean is available for the period prior to the onset of large-scale bomb-production of tritium (March 1954), the comparison is made as follows. Using extreme values of 0.5 and 1.5 T atoms/cm²/sec for the rate at which tritium is added to the troposphere (based on the estimates given by *Begamann and Libby* [1957], 1.0 T atoms/cm²/sec; *Craig* [1957*b*], 1.2 T atoms/cm²/sec; *Giletti, Bazan, and Kulp* [1958], 0.75 T atoms/cm²/sec and *Bolin* [1958], 0.9 ± 0.2 T atoms/cm²/sec), an upper and lower limit for the tritium concentration in the various oceanic reservoirs can be made. Three assumptions are required: (1) of the total tritium added to the troposphere, 90 per cent ultimately reaches and decays in the oceans; (2) tritium is added to the ocean in a geographically uniform manner; (3) the tritium cycle was at steady state prior to 1954.

The results of this calculation are given in Table 8 along with averages of the existing data. For both the North Atlantic and the Pacific-Indian surface reservoirs the measured values fall just beyond the allowed range. Because of the uncertainties in the production rate and in assumptions 2 and 3, the agreement may be considered satisfactory, suggesting that the thicknesses and residence times of water in the surface reservoirs are realistic.[2]

---

[2] Since the preparation of this paper, Craig and Lal (private communication) have suggested that the tritium production rate is actually as low as 0.35 T atoms/cm²/sec. If this is the case, it is difficult to explain the high concentrations of tritium found in the surface ocean by *Begamann and Libby* [1957] and by *Giletti, Bazan, and Kulp* [1958]. The lack of agreement between the production rate estimates and the surface inventories is made far worse if vertical mixing between the surface and central waters is as rapid as would be suggested by *Bowen and Sugihara's* [1960] Sr^{90} data. The uncertainties introduced by these recent developments remove the value of tritium data as a check on the circulation model proposed here.

A second independent test of the model is to compare the measured reduction in the C^{14}/C^{12} ratio in atmospheric CO_2 resulting from the addition of fossil CO_2 to the system with the reduction predicted by the steady-state model. The predicted decrease is based on the estimates of fossil CO_2 production given by *Suess and Revelle* [1957] for 10-year periods beginning in 1860 and on the following assumptions: (1) the excess CO_2 added to the system does not measurably (± 10 per cent) alter the transfer rate of CO_2 between the ocean and atmosphere; (2) the CO_2 in the atmosphere equilibrates isotopically with the living terrestrial biosphere within a few years but does not equilibrate measurably (± 10 per cent) with the humus of terrestrial soils in the time available (~ 30 years). Because the seven simultaneous differential equations involved in this calculation are not readily solved, the calculation has been carried out numerically. The rate at which C^{14} added instantaneously to one reservoir (the atmosphere) mixes into the other reservoirs is first determined. The fossil CO_2 may be considered a series of negative C^{14} spikes added to the system at various times between 1860 and 1955. The degree of mixing of each of these spikes can then be determined for any given time after addition. The sum of the contribution of each spike yields the net effect in a given reservoir for any given time between 1860 and 1955. The results are plotted in Figure 7 along with the best estimate of the actual reduction based on C^{14} measurements on tree rings [*Suess*, 1955; *Brannon, Daughtry, Perry, Whitaker, and Williams*, 1957; *Fergusson*, 1958; *Munnich and Vogel*, 1958; *Hayes, Anderson, and Arnold*, 1955]. Whereas Fergusson's data appear to be the most definitive, the consistently higher estimates obtained by the other authors have been given weight by increasing all Fergusson's reduction estimates by 25 per cent. The double arrow in the diagram represents the uncertainty in the estimates based on tree ring data. The curve for no exchange between the fossil CO_2 and the carbon of reservoirs other than the atmosphere is given for comparison. Whereas the predicted curve yields a somewhat greater reduction than has been observed, the two estimates are sufficiently close so that the difference could result from errors in the assumptions (particularly the one con-
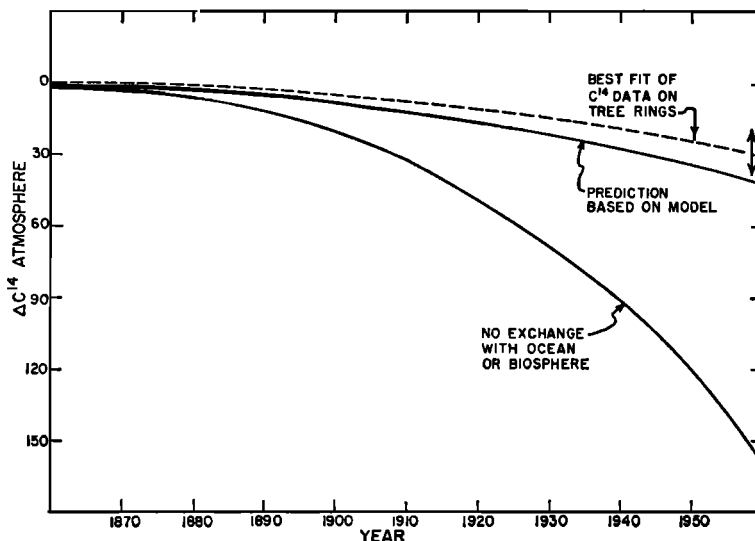
Fig. 7. Changes in the C^{14}/C^{12} ratios of atmospheric CO_2 resulting from dilution with industrial CO_2. The dashed curve is based on the 25 ± 10 per mil reduction suggested by tree ring data (see text), and the upper solid curve is based on CO_2 production estimates and the steady-state model. The double arrow indicates an estimate of the uncertainty in the experimental curve.

cerning the exchange with the humus reservoir) rather than weaknesses in the steady-state model. Again the thickness of and residence time of water in the surface reservoirs largely control the prediction.

Bolin and Eriksson [1959] recently made a similar prediction of the effect of fossil CO_2 on the C^{14}/C^{12} ratio in atmospheric CO_2 by using the three-layer model referred to above. Selecting values of their parameters τ_{A-M} and τ_{D-M} corresponding to a ΔC_{SW}^{14} of -43 per mil and a ΔC_T^{14} of -160 per mil, the predicted decrease in atmospheric C^{14}/C^{12} ratio would be about 6 per cent in 1954 compared with about 4 per cent based on the more complex model used in this paper. The reason for this difference is not apparent. ·

The deep water masses act as infinite reservoirs for both radiocarbon and tritium. In one case more than adequate amounts of C^{14} can be returned to the atmosphere without altering the C^{14}/C^{12} ratio of the deep reservoirs, and in the other case all the tritium in the system could be added to the deep water reservoirs without creating a significant return flux to the surface.

A potential third test of the model would be to observe the distribution of bomb-produced C^{14} in the system. Again the test will be mainly on the characteristics of the surface water reservoirs. Whereas up to 1958 the magnitude of the bomb effect in the oceans was so small that precise experimental estimates were not obtained, *Broecker and Olson* [in press] have shown that the results obtained are consistent with the increase predicted by the model. Within a few years the effect will be of such magnitude that precise measurement will be possible.

Besides the tests provided by the distribution of tritium and the fossil CO_2 effect, the case for the steady-state model is to some extent fortified because certain features of the C^{14} distribution itself can be predicted. The rather low ΔC^{14} values obtained for Antarctic surface water samples are a natural result of the continual addition to this reservoir of low C^{14} water from the Atlantic and Pacific-Indian deep reservoirs to the vertically mixed Antarctic reservoir. Although more tenuous, the increase in ΔC^{14} from the Antarctic to the South Atlantic to the Caribbean to the North Atlantic to the Arctic can be explained by progressive equilibration with the atmosphere as water is transported from south to north along the Atlantic surface. The Arctic reservoir could well show a reversal in this trend if a major portion of the water re-

TABLE 9. Distribution of C^{14} in the Ocean-Atmosphere System if the Oceanic Mixing Rates (R_i) Were Double or Half the Computed Values (L is held constant.)

Reservoir	Observed ΔC^{14}, ‰	Predicted ΔC^{14} if $R_i' = 2R_i$, ‰	Predicted ΔC^{14} if $R_i' = \frac{1}{2}R_i$, ‰
1	0	0	0
2	−32	−32	−20
3	−46 (−65)*	−66	−49
4	−35	−45	−18
5	−200	−145	−280
6	−113 (−120)*	−90	−135
7	−104	−85	−155
8	−28 (−30)*	−50	−21

* Estimates based on model.

turning to the surface from the Atlantic deep water system were returned to this reservoir instead of to the Antarctic. The higher Arctic value obtained by *Fonselius and Ostlund* [1959] (see Tables 2 and 4) thus lends support to the 'cycle' pattern for the Atlantic circulation as opposed to the 'exchange' pattern for the Pacific circulation.

Since with the exception of L no errors are attached to the estimates of the rates determined on the basis of the model, it is of interest to examine the sensitivity of these unknowns to the parameters selected. One way to approach this problem is to compare the steady-state ΔC^{14} values predicted by the model if the three rates (R_i) were twice (or half) the values given in Table 7 with the observed ΔC^{14} values. This has been done in Table 9. The results have been normalized so that the atmospheric ΔC^{14} value is zero in each case. The absolute C^{14}/C^{12} ratio in the atmosphere would be 7 per cent lower than it is at present in the first case and 8 per cent higher in the second. Inspection of these results indicates that if the rates were changed by 50 per cent, a significant deviation between the measured and computed ΔC^{14} values for reservoirs 5, 6, and 7 would exist.

It is also necessary to consider the sensitivity of the model to changes in the thickness of the mixed layer. It is possible that the Central Water systems should at least in part be included in the mixed layer rather than entirely in the deep reservoirs. In this case the effective thickness of the surface reservoirs could be as great as 300 meters. As L is independent of the oceanic mixing model selected, it remains unchanged. Examination of the steady-state equations shows that R_1, R_2, R_3, x_4, x_6, and x_3 are also essentially independent of this depth. The mean residence times given in Figure 6 for the surface reservoirs (2, 3, and 4) become three times as great. This results in a change from a predicted value of 35 per mil for the industrial CO_2 effect to a value of approximately 22 per mil. In the case of the tritium concentrations it would reduce the predicted values by a factor of slightly more than 2 for both the North Atlantic and Pacific surface water reservoirs. Thus, increasing the depth of the surface reservoirs brings the predicted and observed industrial effects closer together but drives the predicted and observed tritium concentrations farther apart. C^{14} data from future bomb tests should be very useful in this respect, as it will provide a third independent test.

Although the steady-state model given here incorporates only the gross features of large-scale circulation, it may prove useful in certain types of investigations. The rate of mixing of bomb-produced C^{14} with oceanic CO_2, the rate of oxygen consumption in the deep ocean, the uptake of industrial CO_2 by the oceans, and the rate of interoceanic mixing are examples of problems which require a model of this type. Because of the restriction to problems involving time scales of more than 100 years, the natural radiocarbon method is far better suited to these large-scale problems than to detailed studies of mixing within a given local reservoir.

Nonsteady-state models. If mixing within the oceans occurs discontinuously on a time scale of tens to hundreds of years, results based on steady-state assumptions could be seriously in error. As an example a hypothetical case is demonstrated in Figure 8. It is assumed that the ocean mixes very rapidly during alternate 100-year periods. During the intervening 100-year periods no mixing occurs between the water above and below 100 meters in the ocean. The exchange rate between the atmosphere and the surface of the ocean is assumed to be unaltered by the factors causing the oceanic mixing rate to change. As shown in the figure, the atmos-
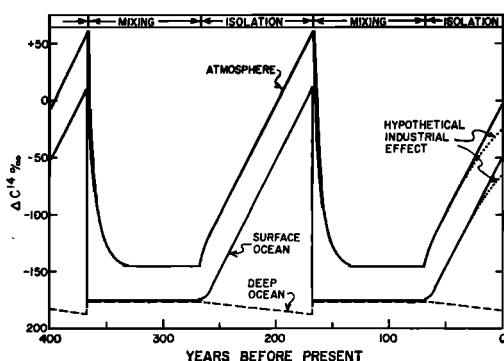
Fig. 8. A hypothetical example of the effects of nonsteady-state mixing on the distribution of C^{14} in the ocean-atmosphere system. One-hundred-year periods of very rapid oceanic mixing are separated by 100-year periods during which no mixing occurs between the upper 100 meters of the ocean and the deep sea. The distribution of C^{14} at $t = 0$ corresponds roughly to that of the present (corrected for industrial CO_2 and bomb-produced C^{14}).

Fig. 9. Steady-state ΔC^{14} values for atmospheric CO_2 as a function of the transfer rate adopted for the oceanic mixing model. The three oceanic mixing rates are assumed to change by the same fraction. The maximum range of observed variations in the ΔC^{14} value for the atmosphere over the last 1000 years is indicated by the vertical arrow and the corresponding maximum range of transfer rates by the horizontal arrow.

phere and surface oceans undergo large changes in ΔC^{14} while the deep oceans show little change. The gradual rise in ΔC^{14} during the isolation period is the result of storage of newly produced C^{14} in the relatively small atmospheric and surface ocean reservoirs. The sharp fall at the onset of mixing is the result of the transfer of this C^{14} into the much larger deep ocean reservoir. Note that the zero on the ΔC^{14} scale is placed 175 per mil above the oceanic average corresponding to the present atmospheric value (corrected). Thus if the oceans were mixing in this hypothetical manner the present distribution would correspond to $t = 0$ on the time scale of the figure.

The importance of this example is that it demonstrates the sensitivity of the atmospheric ΔC^{14} value to changes in oceanic mixing rates. As pointed out by *Broecker* [1957] and by *deVries* [1958], measurement of the C^{14}/C^{12} ratio in tree rings of known growth date (providing estimates of the ΔC^{14} value of the atmosphere at times in the past) should place limits on the extent of nonsteady-state mixing in the oceans.

Measurements available to date [*deVries*, 1958; *Ostlund*, 1957; *Munnich and Vogel*, 1958; *Broecker, Olson, and Bird*, 1959; *Willis, Tauber, and Munnich*, 1960] indicate that the atmospheric C^{14}/C^{12} ratio has
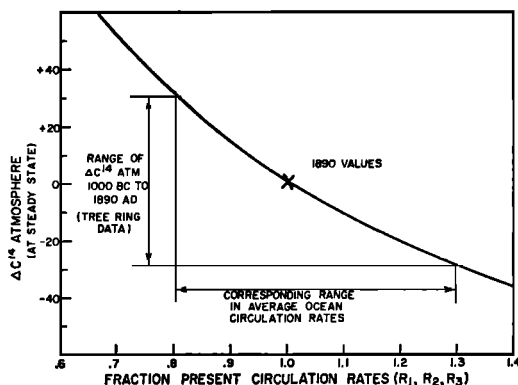
remained within ±25 per mil of its 19th century value during the past 1000 years. There is a strong suggestion that real cyclic variations have occurred within these limits. Since part or even all of the observed variation could be the result of variations in the production rate of C^{14}, no definite conclusions regarding oceanic circulation variations can be made. It is possible, however, to place an upper limit on the amount of large-scale nonequilibrium circulation that has occurred over the past 1000 years. As shown in Figure 9, in order to produce the range of observed variations in atmospheric ΔC^{14}, the rates R_1, R_2, and R_3 in the steady-state model would have to be varied only about 30 per cent on either side of the present values (assuming that the three rates undergo the same fractional change). It should be emphasized that, whereas the atmosphere is a sensitive indicator of large-scale variations in oceanic circulation rates, large changes in the rate for one local reservoir would not be detectable by this approach.

Summary. Although tree ring data suggest that the average turnover rate for the ocean has been relatively constant during the past 1000 years, it is not possible to state with any certainty whether any given local reservoir is at steady state. Because of the small volume

of the Atlantic Ocean compared with that of the Pacific and Indian Oceans it could well be considered a local reservoir. Thus it is entirely possible that part of the difference in the ΔC^{14} values of surface and deep water in the Atlantic is the result of storage of newly produced C^{14} in the surface layers (Fig. 8) rather than to radioactive decay, as was assumed in the steady-state calculations. In this sense the steady-state estimates represent upper limits on the deep water residence times.

Conclusions. The results presented in this paper clearly demonstrate the value of the radiocarbon method in oceanographic studies. When used in conjunction with the proper oceanographic information and with other isotope data (H^3, Si^{32}, Ra^{226}, Sr^{90}, . . .), C^{14} data will provide estimates of the large-scale mixing rates within the ocean. As many questions remain unanswered, the time estimates given here must be considered tentative. Perhaps the main value of the paper is that it (1) provides a broad base for more detailed future investigations, (2) demonstrates to some extent the potentialities as well as the limitations of the natural radicarbon method in studies of oceanic circulation, and (3) points out some of the main problems requiring solution before more reliable time estimates can be made.

REFERENCES

Arnold, J. R., and E. C. Anderson, The distribution of C^{14} in nature, *Tellus, 9,* 28–32, 1957.

Begamann, F., and W. F. Libby, Continental water balance, ground-water inventory, and storage times, surface ocean mixing rates and world-wide water circulation patterns from cosmic ray and bomb tritium, *Geochim. et Cosmochim. Acta, 12,* 277–296, 1957.

Bolin, B., On the use of tritium as a tracer for water in nature, *Second United Nations Intern. Conf. on the Peaceful Uses of Atomic Energy, 18,* 336–343, 1958.

Bolin, B., and E. Eriksson, Changes in the carbon dioxide content of the atmosphere and sea due to fossil fuel combustion, *Rossby Memorial Volume,* Rockefeller Inst. Press, New York, 130–142, 1959.

Bowen, V. T., and L. T. Sugihara, Strontium-90 in the "mixed layer" of the Atlantic Ocean, *Nature, 186,* 71–72, 1960.

Brannon, H. R., A. C. Daughtry, D. Perry, W. W. Whitaker, and M. Williams, Radiocarbon evidence on the dilution of atmospheric and oceanic carbon by carbon from fossil fuels, *Trans. Am. Geophys. Union, 38,* 643–650, 1957.

Brodie, J. W., and R. W. Burling, Age determinations of southern ocean waters, *Nature, 181,* 107–108, 1958.

Broecker, W. S., Application of radiocarbon to oceanography and climate chronology, Ph.D. Thesis, Columbia University, 1957.

Broecker, W. S., W. M. Ewing, R. Gerard, B. C. Heezen, and J. L. Kulp, The significance of variations of light isotope abundances in oceanographic studies, *Natl. Acad. Sci. Natl. Research Council Publ. 572,* 118–134, 1958.

Broecker, W. S., and E. A. Olson, Lamont radiocarbon measurements, 6, *Am. J. Sci. Radiocarbon Suppl., 1,* 111–132, 1959.

Broecker, W. S., and E. A. Olson, Further information on radiocarbon from nuclear tests, *Science,* in press.

Broecker, W. S., E. A. Olson, and J. Bird, Radiocarbon measurements on samples of known age, *Nature, 183,* 1582–1584, 1959.

Broecker, W. S., C. S. Tucek, and E. A. Olson, Radiocarbon analysis of oceanic CO_2, *Appl. Radiation and Isotopes, 7,* 1–18, 1959.

Broecker, W. S., and A. Walton, Radiocarbon from nuclear tests, *Science, 130,* 309–314, 1959a.

Broecker, W. S., and A. Walton, The geochemistry of C^{14} in fresh-water systems, *Geochim. et Cosmochim. Acta, 16,* 15–38, 1959b.

Burling, R. W., and D. M. Garner, A section of C^{14} activities of sea water between 9°S and 66°S in the southwest Pacific Ocean, *New Zealand J. Geol. Geophys.,* in press.

Craig, H., The geochemistry of the stable carbon isotopes, *Geochim. et Cosmochim. Acta, 3,* 53–92, 1953.

Craig, H., The natural distribution of radiocarbon and the exchange time of carbon dioxide between atmosphere and sea, *Tellus, 9,* 1–17, 1957a.

Craig, H., Distribution, production rate, and possible solar origin of natural tritium, *Phys. Rev., 105,* 1125–1127, 1957b.

deVries, H., Variation in concentration of radiocarbon with time and location on earth, *Koninkl. Ned. Akad. Wetenschap. Proc., Ser. B, 61*, 1–9, 1958.

Fergusson, G. J., Reduction of atmospheric radiocarbon concentration by fossil fuel carbon dioxide, *Proc. Roy. Soc. London, A, 243*, 561–574, 1958.

Fonselius, S., and G. Ostlund, Natural radiocarbon measurements on surface water from the North Atlantic and the Arctic Sea, *Tellus, 11*, 77–82, 1959.

Garner, D. M., A radiocarbon profile in the Tasman Sea, *Nature, 182*, 466–468, 1958.

Giletti, B. J., F. Bazan, and J. L. Kulp, The geochemistry of tritium, *Trans. Am. Geophys. Union, 39*, 807–818, 1958.

Hayes, F. N., E. C. Anderson, and J. R. Arnold, Liquid scintillation counting of natural radiocarbon, *Intern. Conf. on the Peaceful Uses of Atomic Energy, 14*, 188–192, 1955.

Kulp, J. L., L. E. Tryon, W. R. Eckelmann, and W. A. Snell, Lamont natural radiocarbon measurements, 2, *Science, 116*, 409–414, 1952.

Munnich, K. O., and J. C. Vogel, Radioactive carbon in the atmosphere produced by atomic explosions, *Naturwissenschaften, 14*, 327–329, 1958.

Ostlund, H. G., Stockholm natural radiocarbon measurements, 1, *Science, 126*, 493–497, 1957.

Rafter, T. A., C^{14} variations in nature and the effect on radiocarbon dating, *New Zealand J. Sci. Technol., B, 37*, 20–38, 1955.

Rafter, T. A., and G. J. Fergusson, Atmospheric radiocarbon as a tracer in geophysical circulation problems, *Second United Nations Intern. Conf. on the Peaceful Uses of Atomic Energy, 18*, 526–532, 1958.

Rubin, M., and C. Alexander, U. S. Geological Survey radiocarbon dates, 4, *Science, 127*, 1476–1487, 1958.

Stommel, H., A survey of ocean current theory, *Deep-Sea Research, 4*, 149–183, 1957a.

Stommel, H., Toward a future study of the abyssal circulation, Symposium on abyssal circulation, IUGG, Toronto Meeting, 1957b.

Stommel, H., The abyssal circulation, *Deep-Sea Research, 5*, 80–82, 1958.

Suess, H. E., Radiocarbon concentration in modern wood, *Science, 122*, 415–417, 1955.

Suess, H. E., N. W. Rakestraw, and H. Oeschger, Apparent age of deep water in the Pacific Ocean, *Preprints, Intern. Oceanog. Congr.*, p. 440, 1959.

Suess, H. E., and R. Revelle, Carbon dioxide exchange between atmosphere and ocean and the question of an increase of atmospheric CO_2 during the past decades, *Tellus, 9*, 18–27, 1957.

Sverdrup, H. U., Oceanography, chap. 5, in *The Earth as a Planet*, edited by G. P. Kuiper, Univ. Chicago Press, 1954.

Sverdrup, H. U., M. W. Johnson, and R. H. Fleming, *The Oceans*, Prentice-Hall, Inc., New York, 1942.

Swallow, C., and L. V. Worthington, Measurements of deep currents in the western North Atlantic, *Nature, 179*, 1183–1184, 1957.

Willis, E. H., H. Tauber, and K. O. Munnich, Variations in the atmospheric radiocarbon concentration over the past 1300 years, *Am. J. Sci. Radiocarbon Suppl., 2*, 1–4, 1960.

Wüst, G., Die Stratosphäre, Deutsche Atlantische Exped. *Meteor 1925–1927, Wiss. Erg., Bd. 6, Teil, 2. Lief.*, 288 pp., 1935.

Wüst, G., Quantitative Untersuchungen zur Statik und Dynamik des Atlantischen Ozeans, Deutsche Atlantische Exped. *Meteor 1925–1927, Wiss Erg., Bd. 6, 2 Tiel, 6. Lief.*, 261–420, 1957a.

Wüst, G., On the meridional volume transport within different strata of the South Atlantic, especially in abyssal depths, Symposium on Abyssal Circulation, IUGG, Toronto Meeting, 1957b.